

# Optical Manipulation of Quantum Dot Electron Spin Qubits Using Microcavity Quantum Well Exciton-Polaritons.

Shruti Puri<sup>1</sup>, Peter L. McMahon<sup>1</sup> and Yoshihisa Yamamoto<sup>1,2</sup>

1. *E. L. Ginzton Laboratory, Stanford University, Stanford, California 94305, USA and*

2. *National Institute of Informatics, 2-1-2 Hitotsubashi, Chiyoda-ku, Tokyo 101-8430, Japan*

(Dated: December 6, 2024)

In this paper, we develop and analyze a hardware platform for a scalable quantum computer based on semiconductor quantum dot (QD) electron spin qubits and their Coulomb exchange interaction with microcavity quantum well (QW) exciton-polaritons. This approach is based on the framework of the previously proposed QuDOS architecture (Quantum Dots with Optically Controlled Spins) for surface code quantum computation<sup>1</sup>. Despite the developments in techniques for implementing quantum non-demolition (QND) measurement and nearest-neighbor gates in the QD electron spin system, achieving the resource requirements for fault-tolerance still remains a challenge. In order to overcome this, our scheme relies on the indirect optical control of QD spins, resulting from the long-ranged Coulomb exchange interaction between the spin qubits and optically excited, spin-polarized, QW exciton-polaritons. We develop schemes for implementing a fast, high-fidelity, single qubit gate, a two-qubit geometric phase gate and single-shot QND measurement. The control mechanism, namely, the exchange interaction, enables the optical manipulation of single electron spin in Faraday geometry. Furthermore, we investigate various decoherence mechanisms critical for the robustness of the gate operations. This paper, introduces the first plausible polariton-based on-chip hardware platform that could support universal, fault-tolerant operations for implementing large-scale quantum algorithms.

## I. INTRODUCTION

An attractive platform for large-scale quantum computation using surface code error correction, must meet the threshold requirements for fault-tolerant operation. For a system using spins as qubits in optically active quantum dots, the requirements for factoring a 1024-bit integer are: are<sup>1</sup> (i) 2D array of  $10^8$  physical qubits (ii) error probability after each gate operation  $< 1\%$  and (iii) gate time and measurement time  $\sim 10$ 's of ns. Quantum dots (QDs) with optically controlled spins (QuDOS) are promising candidates for a scalable implementation of quantum computation. With advances in fabrication technology, it could be possible to grow large arrays of site-controlled QDs<sup>2</sup>. The complete ultrafast optical control of a single electron spin in a charged QD has been demonstrated using a broadband laser pulse<sup>3,4</sup>. A two-qubit gate, on the other hand, requiring an interaction between two neighboring electron spins is yet to be implemented. One approach is based on the dispersive interaction of cavity photons with two electron spins<sup>5,6</sup>. However, high cooperativity factor ( $C > 10^3$ ) is required to reach error rates below the threshold for fault-tolerant operation ( $C \propto \frac{Q}{V}$ , where  $Q$  is the cavity quality factor and  $V$  is the mode volume). Although a planar microcavity is infinite in extent, the cavity modes have a finite transverse extent<sup>7,8</sup>. The inherent mode radius in a planar microcavity is:  $R = \sqrt{\lambda L_c / 2\pi(1 - r_1 r_2)}$ , where  $\lambda$  is the optical wavelength,  $L_c$  is the effective cavity length and  $r_1(r_2)$  is the reflectivity of the top(bottom) mirror<sup>9</sup>. If the mirror reflectivities are increased to increase  $Q$ ,  $R$  also increases, making it difficult to achieve a high cooperativity factor in planar microcavities. Another challenge

is the fast, high fidelity, single-shot measurement of the qubit state. The measurement scheme considered in QuDOS is based on Faraday rotation using dispersive cavity-spin interaction<sup>10</sup>. This technique suffers from measurement backaction: the probe pulse can also lead to spin-flip Raman transitions (with probability  $\propto 1/C$ ). Recently, a single-shot readout of a QD spin was demonstrated<sup>11</sup>. The measurement scheme relied on efficient collection of fluorescence from a pseudo-cycling transition. The measurement was carried out within 800 ns, but the fidelity was limited to 82%. Thus, it seems desirable to decouple the optical transitions for state preparation, manipulation and measurement. This can be achieved in a QD molecule and indeed quantum jumps have been observed in two vertically stacked InAs QDs<sup>12</sup>. However, the measurement is slow ( $\sim 2$  ms) and the probability for the spin to flip is  $\sim 7\%$ . Furthermore, QD molecules are not suited for scaling to large number of qubits because of difficulty in achieving spectral homogeneity. In order to address the outstanding challenges of achieving fast, high fidelity, QND measurement and two-qubit operation, we propose to use Coulomb exchange interaction between QD electron spins and optically excited, quantum well (QW) microcavity exciton-polaritons. The strength of this scheme is twofold. Firstly, by a careful design of the QW and QD it is possible to separate the optical field from the QD manifold, thus preventing any unwanted backaction during a measurement event. Secondly, the bosonic nature of polaritons and their weak interaction with the solid-state environment allows the injection of numerous polaritons coherently in a single mode, increasing the nonlinearity in the qubit-polariton coupling, crucial for two-qubit operation.

Previously, a scheme for a two-qubit gate for electron spins in electrostatic QDs using QW exciton polaritons was proposed<sup>13</sup>. However, the challenge of exciting QW polaritons in the presence of electric fields required to define the QD has not been addressed. A more practical realization was later introduced<sup>6</sup> for implementation of a QND measurement, which predicts a single-shot readout fidelity of 99.9%. However, the required measurement time is  $\tau_{\text{meas}} \sim 10$  ns is still an order of magnitude slower than the fastest single-shot measurement operation demonstrated<sup>11</sup>. In this paper, we improve upon the previous proposal by introducing “traps” to confine QW polaritons. This confinement leads to an increase in the Coulomb exchange energy and eliminates the dependence between  $Q$  and  $R$ . In this new setup, we develop schemes for implementing a fast, high-fidelity, single qubit gate, a two-qubit geometric phase gate and single-shot QND measurement. We would like to emphasize that our proposals for all three of these operations function the in Faraday geometry. Thus, the indirect optical control and manipulation of the QD spin qubits using their exchange interaction with the QW polaritons provides a scalable platform for the implementation of fault-tolerant quantum logic gates.

## II. SETUP

The system we propose operates in the Faraday geometry, so that the QD electron spin is quantized along the growth ( $z$ ) axis by an external magnetic field  $B_0 \hat{z}$ . As illustrated in Fig. 1(a), the setup consists of a 2D array of  $\text{In}_x\text{Ga}_{1-x}\text{As}$  QDs grown on top of a  $\text{In}_y\text{Ga}_{1-y}\text{As}$  QW, with a few-monolayer-thick GaAs barrier in-between them. The QDs and QW are embedded in a GaAs  $\lambda$  cavity formed by AlGaAs/AlAs distributed Bragg mirrors (DBRs). The GaAs spacer region is etched before the growth of the top DBR, creating a locally ( $\Delta\lambda_c \sim 5$  nm) thicker cavity (Fig. 1(b)). The length of the cavity in the etched region is  $\lambda_c$  and that in the spacer is  $\lambda_c - \Delta\lambda_c$ . The lowest resonance frequency in the spacer is  $\sim \omega_t = \frac{2\pi c \Delta\lambda_c}{n\lambda_c L_c}$ <sup>15,16</sup>, where  $L_c$  is the cavity length. This local modulation of cavity length introduces a microscale trap potential ( $\hbar\omega_t = 7$  meV) for cavity photons. The trap radius  $R$  is defined by electron-beam lithography<sup>17,18</sup>. The photons outside the trap region are non-resonant with the cavity and have an extremely short lifetime. In the etched region, the QW exciton is resonant with the lowest cavity photon mode ( $\mathbf{k}_{\parallel} = \mathbf{0}$ ) and in the strong coupling regime, the resulting eigenmodes of the system are upper polaritons (UPs) and lower polaritons (LPs)<sup>15,17–19</sup>. The splitting between the UP-LP mode ( $2\Omega_R$ ) depends on the strength of the dipole coupling between the QW excitons and cavity photons. Typically, in a single QW  $2\Omega_R \sim 3\text{--}4$  meV. As a result, the confinement of photons also leads to confinement of polaritons. For a potential depth of 7 meV,  $R = 1$   $\mu\text{m}$  and photon confine-

ment strength is 1.5 meV, which is smaller than the rate at which the photon and exciton exchange energy ( $2\Omega$ ). Thus, the polariton can be considered as a particle with effective mass  $m_p$ , placed in a lateral potential trap. The lateral confinement results in the discretization of the energy-momentum dispersion,  $E = E_0 + \frac{\hbar^2 |\mathbf{k}_{\parallel}|^2}{2m_p}$ , where  $\mathbf{k}$  is the quantized in-plane momentum vector. The angle-resolved photoluminescence spectrum from the emission from the ground state in such a trap will be peaked around  $\mathbf{k}_{\parallel} = \mathbf{0}$ . Thus we will refer to the ground state mode as the  $\mathbf{k}_{\parallel} = \mathbf{0}$  mode. In planar DBR cavities with no local modulation of cavity length, the polaritons are delocalized over the region with radius equal to mode radius in the cavity. Thus, lateral confinement of polaritons in smaller regions without loss in cavity  $Q$  leads to increase in the strength of their interaction with the QD spin qubit (for details see section slowromancapiv@ and reference 14). In the cavity described above, the splitting between the ground state and first excited state of the LP is  $\sim 1$  meV. Thus, a red-detuned ( $\delta$ ), left(right) circularly polarized  $\{\sigma^+(\sigma^-)\}$  laser pulse excites  $\mathbf{k}_{\parallel} = \mathbf{0}$  LPs in the trap region of area  $A$  below the QDs. Because of the QW exciton selection rules, LPs with total angular momentum along the growth direction  $J_z = +1(-1)$  and  $\mathbf{k}_{\parallel} = \mathbf{0}$  are excited<sup>20</sup>. The excitonic component of the LP is composed of an electron with  $s_{ze} = -\frac{1}{2}(+\frac{1}{2})$  and a heavy-hole with  $l_{zhh} = +1(-1)$ ,  $s_{zhh} = +\frac{1}{2}(-\frac{1}{2})$ , where  $s$  and  $l$  refer to spin and orbital angular momentum<sup>21,22</sup>. Excitons with  $s_{ze} = +\frac{1}{2}(-\frac{1}{2})$ ,  $l_{zhh} = +1(-1)$  and  $s_{zhh} = +\frac{1}{2}(-\frac{1}{2})$  are optically dark states and are blue detuned ( $\sim 1.5\text{--}2$  meV) from the  $\mathbf{k}_{\parallel} = \mathbf{0}$  LP mode.

## III. TUNNEL COUPLING BETWEEN NEIGHBORING TRAPS

Our aim is to use the optically excited QW LP mode to control and manipulate the QD electron spin qubits. For controlling a single electron spin trapped in a QD, LPs must be excited in the trap under that QD. However, a two-qubit operation requires two coupled  $\mathbf{k}_{\parallel} = \mathbf{0}$  LP modes in the traps under two adjacent QDs. Thus, it is crucial to have a strong coupling between the LP modes in neighboring traps which are typically separated by a distance  $D$  ( $D >$  diffraction limit of the optical pulse). The in-plane effective mass of LPs ( $1/\mathbf{m}_{\text{eff}} = d^2 E(\mathbf{k}_{\parallel})/d^2 \mathbf{k}_{\parallel}$ ) is  $\sim 10^3$  smaller than that of excitons<sup>23</sup>. Consequently, it is possible to achieve a strong tunnel coupling between the two LP modes even when  $D \sim 1\text{--}2$   $\mu\text{m}$ . The Hamiltonian for this linear tunnel coupling between the LP modes in two neighboring traps is given by:

$$\hat{H}_{\text{t.c.}} = \hbar\omega_1 a_1^\dagger a_1 + \hbar\omega_2 a_2^\dagger a_2 + U(a_1^\dagger a_2 + a_2^\dagger a_1)$$

where,  $\hbar\omega_{1(2)}$  is the energy of the LP mode in trap 1(2),  $a_{1(2)}^\dagger$ ,  $a_{1(2)}$  is the creation, annihilation operators for the LP mode in trap 1(2) and  $U$  is the coupling strength.

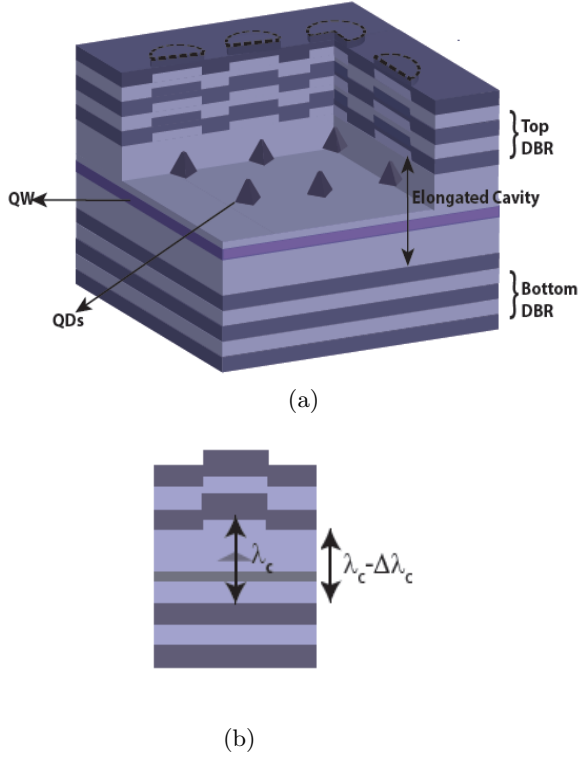


FIG. 1. (a) Illustration of the proposed setup: 2D array of QDs coupled to QW in patterned DBR microcavity. The cavity length is locally modulated to create potential traps for photons. (b) Cross-section of the structure showing the modulation of cavity length<sup>17,18</sup>. Photons are trapped in the circular region where the cavity length equals the wavelength  $= \lambda_c$ . A trap potential  $\sim 7$  meV is created for  $\Delta\lambda_c = 5$  nm.

In the supplement<sup>16</sup>, we outline the method employed for calculating  $U$ . Figure 2(a,b) presents the dependence of  $U$  on  $D$  and the trap width  $2R$ . For the purpose of simplicity and comparing our results with the estimates available in other references<sup>1</sup>, we consider the trap to be a square potential well of side  $2R$  and potential depth of 7 meV. The distance  $D$  is measured from the nearest edge-to-edge separation between the traps (Fig. 2(c)). For example, the coupling strength ( $U$ ) between two traps of half-width  $R = 1 \mu\text{m}$  that are separated by  $D = 0.5 \mu\text{m}$  (or  $2.5 \mu\text{m}$  center-to-center) is  $U = 0.5$  meV. The coupling strength between circular traps should be of the same order of magnitude. A strong coupling between traps is essential for a two-qubit operation, but is detrimental for a single qubit manipulation. Unwanted excitation of LP modes in neighboring traps via tunnel coupling will lead to crosstalk and decoherence of neighboring spins. Next, we explain how this dichotomy can be overcome.

For clarity in presentation, we will only consider the nearest-neighbor coupling. Consider a target trap T, which is directly under the QD that hosts the spin qubit we intend to manipulate. The neighboring traps are numbered 1 – 4 and our aim is to excite a  $\mathbf{k}_{\parallel} = \mathbf{0}$  LP

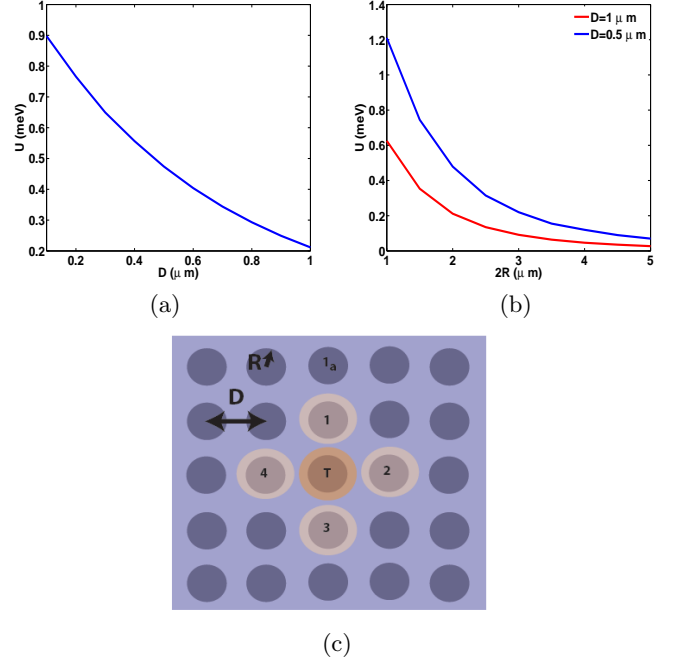


FIG. 2. Variation of  $U$  with (a)  $D$  for  $2R = 3 \mu\text{m}$  (b)  $2R$  for  $D = 1 \mu\text{m}$  (red curve) and  $D = 0.5 \mu\text{m}$  (blue curve). (c) Top view of the structure showing the LP traps (blue circles) and pump laser pulses over the target trap, T ( $F_T$ ) and nearest-neighbor traps 1-4 ( $F$ ). As shown in the main text when  $F = \frac{iF_T U}{i\delta + \frac{\gamma}{2}}$ , LPs are only excited in the target trap.

mode only in trap T (Fig. 2(c)). In order to do so we excite LPs in trap T and the four neighboring traps by a pump  $F_T$  and  $F$  respectively. Both the pumps are red detuned from the  $\mathbf{k}_{\parallel} = \mathbf{0}$  LP mode in the traps by  $\delta$ . In the rotating frame of the pump pulse, the rate equations for the coherent amplitude ( $\alpha_{T(1-4)}$ ) of the  $\mathbf{k}_{\parallel} = \mathbf{0}$  LP mode in trap T(1-4) are given by<sup>16</sup>:

$$\frac{d\alpha_T}{dt} = \sqrt{\gamma_t} F_T - \left(i\delta + \frac{\gamma}{2}\right) \alpha_T - iU \sum_{i=1}^4 \alpha_i, \quad (1)$$

$$\frac{d\alpha_i}{dt} = \sqrt{\gamma_t} F - \left(i\delta + \frac{\gamma}{2}\right) \alpha_i - iU \alpha_T - iU \sum_{k=1}^3 \dots, \quad (2)$$

$i = 1, 2, 3, 4$

where,  $\gamma(\gamma_t)$  is the decay rate of polaritons from the cavity (top mirror),  $|F_T|^2$  ( $|F|^2$ ) is the photon flux in the pump incident on trap T (neighboring traps). The last term in Eqn. 23 represents the coupling of the trap  $i$  with the other neighboring traps. For example, the coherent state evolution in trap  $1_a$  is given by<sup>16</sup>:

$$\frac{d\alpha_{1_a}}{dt} = -\left(i\delta + \frac{\gamma}{2}\right) \alpha_{1_a} - iU \alpha_1 - iU \sum_{k=1}^3 \dots$$

It will be instructive to solve the above equations at steady state, under the assumption that  $|\alpha_T| \gg |\alpha_i|$ . Un-

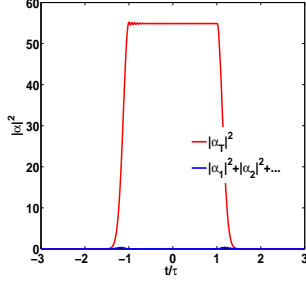


FIG. 3. The number of LPs in trap T  $|\alpha_T|^2$  (red curve) and that in all neighboring traps for (blue curve) as a function of time for  $J = 0.5$  meV,  $\gamma = 0.03$  meV,  $\gamma_t = 0.015$  meV,  $\delta = 0$ ,  $F = \frac{2UF_T}{\gamma}$ ,  $F_T$  as given in Eqn. 4 with  $\sqrt{\gamma_t}F_0 = 0.1$  meV,  $\tau = 200$  ps and  $\tau_F^2 = 50$  ps.

der these conditions, the steady state amplitude of the LP mode in trap T is:

$$\alpha_T = \frac{\sqrt{\gamma_t}F_T}{i\delta + \frac{\gamma}{2}}. \quad (3)$$

By substituting Eqn. 3 into Eqn. 23 we see that if  $F = \frac{iF_T U}{i\delta + \frac{\gamma}{2}}$ , then the effective pump term for LPs in the neighboring traps vanishes. This can be understood as the destructive interference between two possible polaron injection paths in trap  $i$ :

1. Path 1: direct excitation by the pump  $F$ , and
2. Path 2: indirect injection from trap T via tunnel coupling.

Figure 3 plots the average number of LPs in trap T ( $|\alpha_T|^2$ ) and that in the neighboring traps ( $\sum |\alpha_i|^2$ ) for  $U = 0.5$  meV,  $\gamma = 0.03$  meV,  $\delta = 0$ ,  $F = \frac{2UF_T}{\gamma}$  and:

$$\begin{aligned} F_T &= F_0 e^{-\frac{|t+\tau|^2}{\tau_F^2}} \quad \forall \quad t < -\tau, \\ &= F_0 \quad \forall \quad -\tau \leq 0 \leq \tau, \\ &= F_0 e^{-\frac{|t-\tau|^2}{\tau_F^2}} \quad \forall \quad t > \tau. \end{aligned} \quad (4)$$

Here time  $t$  is measured in picoseconds and  $\tau_F$  is the rise time of the pump pulses. We have taken into account all nearest neighbor couplings for a  $5 \times 5$  trap structure i.e., 25 traps with the target trap at the center. If the pulse is long enough and if the rise time  $\tau_F$  is slow enough ( $=50$  ps, in Fig. 3), then LPs are pumped only into the target trap.

To minimize loss of information or decoherence, a single- and two-qubit operation would require off-resonant or virtual excitation of LPs ( $\delta \gg \gamma$ ). In this case only a single pulse over the target qubit, with  $\delta \gg U, \gamma$ , is sufficient. On the other hand, for a QND measurement operation to yield maximum information about the qubit state, the LPs must be excited resonantly (or close to resonance). Thus, to implement the measurement scheme we must employ the above outlined technique to protect the neighboring qubits from decoherence.

#### IV. CONTROL MECHANISM: COULOMB EXCHANGE INTERACTION

A self-assembled  $\text{In}_x\text{Ga}_{1-x}\text{As}$  QD is a pyramidal or lens-like 3D island with a typical height in the range  $\sim 1 - 4$  nm and base width in the range  $\sim 20 - 50$  nm. An  $\text{In}_y\text{Ga}_{1-y}\text{As}$  QW can be grown 4-8 nm thick (the QW thickness  $L$  must be such that  $L \sim a_B$ , where  $a_B$  is exciton Bohr radius). Careful design of the barrier layer thickness and In concentrations ( $x$  and  $y$ ) results in a band structure such that the electron is primarily confined in the QD but has a non-zero wavefunction in the QW. The finite overlap of the localized QD electron and the LPs in the trap directly below the QD, results in a spin-dependent Coulomb exchange interaction between them<sup>25,26</sup>.

$$\begin{aligned} H_I &= -V_{\text{ex},p}^{\mathbf{k}_{\parallel},\mathbf{k}'_{\parallel}} \hat{\sigma}_z a_{1,\mathbf{k}_{\parallel}}^{\dagger} a_{1,\mathbf{k}'_{\parallel}} + V_{\text{ex},p}^{\mathbf{k}_{\parallel},\mathbf{k}'_{\parallel}} \hat{\sigma}_z a_{-1,\mathbf{k}_{\parallel}}^{\dagger} a_{-1,\mathbf{k}'_{\parallel}} \\ &\quad - V_{\text{ex},d}^{\mathbf{k}_{\parallel},\mathbf{k}'_{\parallel}} \hat{\sigma}_z d_{2,\mathbf{k}_{\parallel}}^{\dagger} d_{2,\mathbf{k}'_{\parallel}} + V_{\text{ex},d}^{\mathbf{k}_{\parallel},\mathbf{k}'_{\parallel}} \hat{\sigma}_z d_{-2,\mathbf{k}_{\parallel}}^{\dagger} d_{-2,\mathbf{k}'_{\parallel}} \\ &\quad - V_{\text{ex},f}^{\mathbf{k}_{\parallel},\mathbf{k}'_{\parallel}} \hat{\sigma}_+ a_{1,\mathbf{k}_{\parallel}}^{\dagger} d_{2,\mathbf{k}'_{\parallel}} - V_{\text{ex},f}^{\mathbf{k}_{\parallel},\mathbf{k}'_{\parallel}*} \hat{\sigma}_- d_{2,\mathbf{k}_{\parallel}}^{\dagger} a_{1,\mathbf{k}'_{\parallel}} \\ &\quad - V_{\text{ex},f}^{\mathbf{k}_{\parallel},\mathbf{k}'_{\parallel}} \hat{\sigma}_+ d_{-2,\mathbf{k}_{\parallel}}^{\dagger} a_{-1,\mathbf{k}'_{\parallel}} - V_{\text{ex},f}^{\mathbf{k}_{\parallel},\mathbf{k}'_{\parallel}*} \hat{\sigma}_- a_{-1,\mathbf{k}_{\parallel}}^{\dagger} d_{-2,\mathbf{k}'_{\parallel}} \end{aligned} \quad (5)$$

where,  $\hat{\sigma}_z$  ( $\hat{\sigma}_+$ ,  $\hat{\sigma}_-$ ) are the Pauli spin- $z$  (-raising,-lowering) operator for the QD electron spin,  $a_{i,\mathbf{k}_{\parallel}}^{\dagger}$ ,  $a_{i,\mathbf{k}_{\parallel}}$  ( $d_{i,\mathbf{k}_{\parallel}}^{\dagger}$ ,  $d_{i,\mathbf{k}_{\parallel}}$ ) are the creation, annihilation operators for the LP (dark exciton) with in-plane momentum  $\mathbf{k}_{\parallel}$  and  $J_z = i$ .  $V_{\text{ex},p}^{\mathbf{k}_{\parallel},\mathbf{k}'_{\parallel}}$  ( $V_{\text{ex},d}^{\mathbf{k}_{\parallel},\mathbf{k}'_{\parallel}}$ ) is the magnitude of exchange energy when the spin state of the QD electron and LPs (dark excitons) is conserved, accompanied by the momentum scattering of LPs (dark excitons) with  $\mathbf{k}'_{\parallel}$  into LPs with  $\mathbf{k}_{\parallel}$ . This spin conserving coupling is represented by the first four terms in Eqn.5.  $V_{\text{ex},f}^{\mathbf{k}_{\parallel},\mathbf{k}'_{\parallel}}$  ( $V_{\text{ex},f}^{\mathbf{k}_{\parallel},\mathbf{k}'_{\parallel}*}$ ) is the magnitude of exchange energy when the QD electron flips its spin accompanied by the scattering of a LP with  $J_z = \pm 1$  into a dark exciton state with  $J_z = \pm 2$  (and vice-versa). This spin-flip phenomena is represented by the last four terms in Eqn. 5. The Bloch wavefunction of an electron in the conduction band is s-like, whereas that of a hole in valence band is p-like. As a result, the exchange interaction between the QD electron and QW hole is at least an order of magnitude smaller than that between the two electrons<sup>27</sup>. Therefore, in our analysis the QD electron-QW hole exchange interaction is neglected. We now discuss the consequence of each of the terms in Eqn. 5:

1. The dark excitons with  $J_z = \pm 2$  do not couple with light and the pump pulse only excites LPs. As we mentioned earlier, the dark excitons are blue detuned from the LP resonance. As a result the spin flip terms in Eqn. 5 are non-energy conserving and can be neglected. This is crucial for implementing a QND measurement. This spin-flip mechanism can be made possible by phonon absorption, but the

probability for such a scattering is negligible (section VIII.C).

2. In low density limit the polaritons behave as bosons. The in-plane effective mass of  $\mathbf{k}_{\parallel} = \mathbf{0}$  LPs ( $1/m_{\text{eff}} = d^2 E(\mathbf{k}_{\parallel})/d^2 \mathbf{k}_{\parallel}$ ) is small ( $\sim 4 \times 10^{-5} m_0$ , where  $m_0$  is the free electron mass). In other words, the detuning between the  $\mathbf{k}_{\parallel} = \mathbf{0}$  mode and the first excited state is large ( $\sim 1 \text{ meV} \gg V_{\text{ex}}$ ). Consequently, scattering to higher momentum modes by phonon absorption is negligible. Consequently, a large number of LPs can be pumped in the single  $\mathbf{k}_{\parallel} = \mathbf{0}$  mode, all of which interact coherently with the QD electron spin. However, the density of the LPs ( $n$ ) must be such that interparticle separation is small compared to the scattering length approximated by the exciton Bohr radius ( $a_B$ ). When  $na_B^2 \ll 1$  the polaritons behave as a weakly-interacting Bose gas. In all the calculations in this paper  $na_B^2$  has been limited to  $\leq 10^{-2}$ .

From the arguments presented above it is evident that a normally incident pump, red detuned from the LP resonance coherently excites LPs in the  $\mathbf{k}_{\parallel} = \mathbf{0}$  mode and the interaction Hamiltonian in Eqn. 5 reduces to<sup>13</sup>:

$$H_I = -V_{\text{ex}} \hat{\sigma}_z a_1^\dagger a_1 + V_{\text{ex}} \hat{\sigma}_z a_{-1}^\dagger a_{-1} \quad (6)$$

$$V_{\text{ex}} = |r_0|^2 \int d\mathbf{r}_e d\mathbf{r}_2 d\mathbf{r}_1 \frac{\psi(\mathbf{r}_e, \mathbf{r}_2) \phi(\mathbf{r}_1) e^2 \psi(\mathbf{r}_1, \mathbf{r}_2) \phi(\mathbf{r}_e)}{4\pi\epsilon(|\mathbf{r}_e - \mathbf{r}_1|)}, \quad (7)$$

where  $a_{1,-1}^\dagger (a_{1,-1})$  are the creation (annihilation) operators for the LP mode with  $\mathbf{k}_{\parallel} = \mathbf{0}$ ,  $\epsilon$  is the dielectric constant of the  $\text{In}_y\text{Ga}_{1-y}\text{As}$  QW,  $\mathbf{r}_1, \mathbf{r}_2$  are the position vectors of the electron and hole in the excitonic part of the LP,  $\mathbf{r}_e$  is that of the QD electron,  $\psi$  and  $\phi$  represent the wavefunctions of the excitonic component of the LP and of the localized electron,  $\hat{\sigma}_z$  is the Pauli spin operators of the QD electron.  $r_0$  is the excitonic Hopfield coefficient of  $\mathbf{k}_{\parallel} = \mathbf{0}$  LPs<sup>28</sup>. When the cavity photons and QW excitons are resonant at  $\mathbf{k}_{\parallel} = \mathbf{0}$ ,  $r_0 = 1/\sqrt{2}$ . From Eqn. 6 we see that the exchange interaction induces a spin-dependent shift in the LP resonance. If the QD spin state is  $|s_z\rangle = |\frac{1}{2}\rangle$ , then the resonance energy of a  $J = -1(+1)$  LP will decrease (increase) by an amount  $V_{\text{ex}}$ , making the  $J = 1$  and  $J = -1$  LP non-degenerate. This effect is reversed if  $|s_z\rangle = |-\frac{1}{2}\rangle$ . These spin-dependent shifts of the LP resonance can be employed to achieve qubit operations. From the derivation of the analytic expression for  $V_{\text{ex}}$ <sup>6</sup>, it is possible to see that  $V_{\text{ex}} \propto \frac{1}{A}$ , where  $A$  is the area of the region in which the LPs are excited. The introduction of polariton traps eliminates the dependence between  $A$  and  $Q$  that exists in a planar microcavity (as explained in section 1). As a result, we can obtain a large exchange energy by exciting LPs in a small area without decreasing their lifetime<sup>18</sup>. For the trap described in section II  $A = 2.2 \mu\text{m}^2$ <sup>216</sup>. If  $x = 30\%$ ,  $y = 15\%$ , the size of the QD is  $20 \text{ nm} \times 20 \text{ nm}$

$\times 1.5 \text{ nm}$ , the QW thickness is  $6 \text{ nm}$ , the barrier layer is  $1 \text{ nm}$  thick, then we estimate that  $V_{\text{ex}} \approx 2 \mu\text{eV}$ <sup>6</sup>.

In addition, the photonic part of the LP couples to the QD single electron-trion transition via dipole coupling. For example the photonic part of a  $J = 1$  LP is  $\sigma^+$  polarized and the Jaynes Cummings Hamiltonian representing the dipole coupling between the LP and the QD electron can be written as:

$$\hat{H}_{\text{jc}} = -\Delta \left| \frac{3}{2} \right\rangle \left\langle \frac{3}{2} \right| + gt_0 a_1^\dagger \left| \frac{1}{2} \right\rangle \left\langle \frac{3}{2} \right| + c.c., \quad (8)$$

where  $g$  is the dipole coupling constant,  $\Delta$  is the detuning of the QD electron-trion transition from the LP pump pulse,  $t_0$  is the photon Hopfield coefficient<sup>28</sup>,  $|\frac{3}{2}\rangle$  represents the QD trion state the with  $j_{\text{zh}} = \frac{3}{2}$  and  $s_{ze} = \frac{1}{2}, -\frac{1}{2}$ . Note that the  $\sigma^+$  light does not couple to the  $s_{ze} = -\frac{1}{2}$  states. We propose to design for a sample for which the band structure is such that the QD trion resonance is detuned from the QW exciton resonance by  $\sim 20 \text{ meV}$ . This ensures that the pump pulse is far blue detuned from the QD trion resonance (indicated by the  $-ve$  sign in front of  $\Delta$ ). The off-resonant coupling to the QD single electron-trion transition does not effect the evolution of the LP state to the first order. To the second order, it can lead to a spin-dependent Stark shift ( $= \frac{t_0^2 g_{\ell(r)}^2}{\Delta_{\ell(r)}}$ ) in the LP resonance. In our system we estimate the coupling constant<sup>29</sup>  $g = \sqrt{\frac{e^2 f}{4\epsilon m_0 V}} \sim 60 \mu\text{eV}$  for a oscillator strength  $f \sim 50$ <sup>30</sup> and mode volume  $V = 0.5 \mu\text{m}^3$  (for trap radius  $R = 1 \mu\text{m}$ )<sup>16</sup>. Thus, if a pulse is applied close to the LP resonance and  $t_0 = \frac{1}{\sqrt{2}}$ , then the Stark shift will be  $\sim \frac{(60\mu\text{eV})^2}{2 \times 20\text{meV}} = 0.1 \mu\text{eV} = V_{\text{ex}}/20$ .

## V. EFFECT OF EXTERNAL MAGNETIC FIELD

As we mentioned, an external magnetic field  $B_0$  is applied along the growth (or  $z$ -) axis to define the qubit in Faraday geometry. If  $B_0 = 0$ , then the QD spin qubit's longitudinal relaxation time ( $T_1$ ) is dominated by nuclear hyperfine interaction and  $T_1$  can be as low as  $10\text{-}100 \text{ ns}$ <sup>31</sup>. But as the external magnetic field increases, this relaxation due to coupling with nuclear spins decreases rapidly. There can be some indirect relaxation via coupling to phonon bath (which in our proposal is at  $1.5 \text{ K}$  or  $0.125 \text{ meV}$ ) or spin-orbit coupling. For example,  $T_1 \sim 10 - 20 \text{ ms}$  for an external magnetic field of a few Tesla. However, if the magnetic field increases too much (typically above  $10 \text{ T}$ ),  $T_1$  starts to decrease, because of increase in the phonon density of states<sup>32,33</sup>. On the other hand, the more important timescale in quantum computation is dephasing time  $T_2$  and  $T_2^* (\ll T_1)$ <sup>34</sup>. Due to uncertainty in the nuclear field, the ensemble or time averaged dephasing time ( $T_2^*$ ) is much smaller than the intrinsic dephasing time ( $T_2$ ) and  $T_2^* \sim 4 \text{ ns}$  has been observed<sup>35</sup>. The spin dephasing time can be improved by spin echo techniques and for a magnetic field of  $2 \text{ T}$  a

$T_2 \sim 1 \mu\text{s}$  has been observed in single optical QDs<sup>36</sup>. The external magnetic field also leads to Zeeman and diamagnetic shifts of the  $J = 1$  and  $J = -1$  polaritons<sup>37</sup>. In addition, application of the magnetic field also increases the oscillator strength of the QW excitons due to shrinkage of QW exciton wavefunction<sup>38,39</sup>. However, this effect can be neglected for magnetic fields where the magnetic length  $\ell_B (= \sqrt{\hbar/eB})$  is greater than the exciton Bohr radius. For example, at  $B = 2 \text{ T}$   $\ell_B \sim 20 \text{ nm}$  and hence  $\ell_B > a_B$ . In a  $\text{In}_{0.15}\text{Ga}_{0.85}\text{As}$  QW of width  $\sim 6 \text{ nm}$ , we estimate the splitting between the  $J = 1$  and  $J = -1$  excitons at  $B_0 = 2 \text{ T}$  as  $4V \sim 200 \mu\text{eV}$ <sup>37,40</sup>. The resonant energy of the  $\mathbf{k}_{\parallel} = \mathbf{0}$  cavity photons is such that at  $B = 2 \text{ T}$ , the  $J = 1(-1)$  excitons are red (blue) shifted from the cavity photon resonance by  $2V = 100 \mu\text{eV}$ . As a result the fraction of the excitonic part ( $|r|_0^2$ ) in the LP will increase (decrease) by  $\sim 2\%$  (assuming a vacuum Rabi splitting of  $3 \text{ meV}$  at  $B_0 = 2 \text{ T}$ )<sup>16</sup>. Similarly, the fraction of the photonic part ( $|t|_0^2$ ) in the LP will decrease (increase) by  $\sim 2\%$ . Hence, there will be a small anisotropy in the exchange interaction and dipole coupling of the QD electron with the  $J = 1$  and  $J = -1$  LPs. Furthermore, the  $J = 1$  and  $J = -1$  LPs will be split by an energy  $2V$ . Even in the absence of an external magnetic field, strain-induced asymmetry during the growth process can lift the degeneracy between H- and V-polarized polaritons ( $= 2V_s$ )<sup>41,42</sup>. This leads to spin-scattering of the LPs. Next, we will briefly explain how the effect of Faraday magnetic field and the strain-induced asymmetry is minimized for a two-qubit and single-qubit operation. The effect of non-zero  $V$  and  $V_s$  on the QND readout signal is described in section V of the supplement<sup>6,16</sup>.

As will be described in sections VI and IX,  $J = 1$  ( $J = -1$ ) LPs must be excited using a red-detuned  $\sigma_+$  ( $\sigma_-$ ) pump to implement a two-qubit (single-qubit) gate. The detuning of the pump from the  $J = 1$  ( $J = -1$ ) LPs is  $\delta - V$  ( $\delta + V$ ). The Faraday magnetic field only leads to a renormalization of the LP-pump detuning and is independent of the QD spin state. The fraction of LPs scattered into the  $J = -1$  ( $J = 1$ ) LP mode will be  $\sim \frac{V_s^2}{(\delta+V)^2 + \frac{\gamma^2}{4}} (\frac{V_s^2}{(\delta-V)^2 + \frac{\gamma^2}{4}})$ , where  $\gamma$  is the decay rate of LPs from the cavity<sup>16</sup>. Experimentally, a  $V_s = 150 \mu\text{eV}$  has been measured in planar microcavities<sup>42</sup>. In sections VI and IX, we demonstrate two-qubit and single-qubit operations with  $\delta$  ranging from  $6 - 10 \text{ meV}$ . Hence,  $\delta \gg V, V_s$  and a negligible number of LPs will be scattered from  $J = 1$  ( $J = -1$ ) to  $J = -1$  ( $J = 1$ ) modes. The proposed QND measurement scheme described in section VII requires both  $J = 1$  and  $J = -1$  LPs. Consequently, the Faraday magnetic field will introduce a non-zero baseline signal which can be subtracted from the measurement signal<sup>16</sup>. On the other hand, the strain-induced asymmetry (i.e., non-zero  $V_s$ ) could degrade the signal, leading to increase in measurement time and errors<sup>16</sup> (Table II).

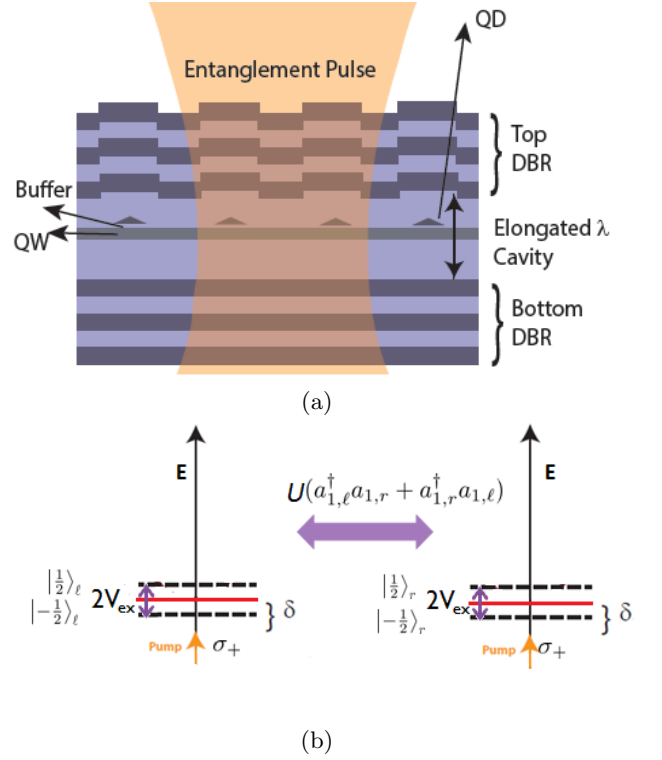


FIG. 4. (a) Illustration of the setup for a two-qubit operation. The pump pulse excites LPs in the trap regions directly below the QDs. (b) Depiction of the LP mode in two traps  $\ell$  and  $r$  and the shift in the LP energy levels by  $2V_{\text{ex}}$  depending on the QD spin states. The horizontal red line shows the LP energy in the absence of the QD electron and the dotted black lines represent the shifted LP energy due to interaction with QD electron.

## VI. TWO-QUBIT GEOMETRIC PHASE GATE

When a state undergoes a cyclic evolution in time under the action of the Hamiltonian  $\hat{H}(t)$ , so that  $\hat{H}(t) = \hat{H}(t + T)$ , it accumulates a geometric phase in addition to the familiar dynamic phase<sup>43</sup>. If the evolution is adiabatic, then the geometric phase depends only on the path that the state follows in parameter space and is called Berry's phase<sup>44</sup>. Under non-adiabatic evolution, the geometric phase, called the Ahranov-Anandan phase, depends only on the path in the projected Hilbert space<sup>45</sup>. Geometric phases are important in quantum computation because they are fault-tolerant to a certain degree<sup>46</sup>. Conditional Berry's phase gate has been demonstrated in NMR experiments<sup>47</sup>. Berry's phase has also been observed in solid-state systems<sup>48</sup>. However due to the requirement of satisfying the adiabatic condition, gates based on Berry's phase are slow. As a result, non-adiabatic geometric gates are more attractive for applications in quantum computation schemes and have been proposed using NMR<sup>49</sup>. In this paper, we propose a two-qubit gate based on the Ahranov-Anandan phase. Figure 4(a) shows a schematic diagram for implement-

ing two-qubit controlled-z operation between neighboring QD spins. A  $\sigma_+$  polarized laser pulse is incident normally on two adjacent QDs. The pulse is red-detuned from the LP ground state at  $\mathbf{k}_{\parallel} = \mathbf{0}$  and virtually excites a coherent population of  $J = 1$  LPs in the traps below the two QDs. If the tunneling rate of polaritons between the traps is  $U$ , then the Hamiltonian for the LPs in the two neighboring traps is:

$$\begin{aligned}\hat{H} = & \delta_{\ell} a_{1,\ell}^{\dagger} a_{1,\ell} + \delta_r a_{1,r}^{\dagger} a_{1,r} \\ & - V_{\text{ex}} \hat{\sigma}_{z,\ell} a_{1,\ell}^{\dagger} a_{1,\ell} - V_{\text{ex}} \hat{\sigma}_{z,r} a_{1,r}^{\dagger} a_{1,r} \\ & - i\sqrt{\gamma_t} P(t) (a_{1,\ell} - a_{1,\ell}^{\dagger} + a_{1,r} - a_{1,r}^{\dagger}) \\ & + U (a_{1,\ell}^{\dagger} a_{1,r} + a_{1,r}^{\dagger} a_{1,\ell}) \\ & + \hat{H}_{\text{jc}},\end{aligned}\quad (9)$$

where,  $a_{1,\ell(r)}^{\dagger}, a_{1,\ell(r)}$  are the creation, annihilation operator for LPs with  $J_z = 1$  in the left- $\ell$  (right- $r$ ) trap,  $\delta_{\ell(r)}$  is the detuning of the  $\mathbf{k}_{\parallel} = \mathbf{0}$  LPs from the pump pulse in the left- $\ell$  (right- $r$ ) trap in the absence of QD electrons,  $|P(t)|^2$  is the photon flux in the pump pulse,  $J$  is the LP tunneling rate in the two traps and  $\hat{H}_{\text{jc}}$  is the dipole coupling Hamiltonian (Eqn. 8). As we mentioned before, this coupling affects the LP resonance only in the second order. Since,  $\frac{g_{\ell(r)}^2}{\Delta_{\ell(r)}} \ll V_{\text{ex}}$  we can neglect the effect of dipole coupling on the LP evolution in comparison to the stronger Coulomb exchange interaction. The effect of the exchange Hamiltonian, depicted in Fig. 4(b). can be interpreted as follows: suppose the spin state of electron in the left QD  $|s_{z,\ell}\rangle = |\frac{1}{2}\rangle$  and that of the electron in the right QD is  $|s_{z,r}\rangle = |-\frac{1}{2}\rangle$ . So the energy of the LP in the left trap will increase by an amount  $V_{\text{ex}}$  and that in the right trap will decrease by an amount  $V_{\text{ex}}$ . On the other hand, if  $|s_{z,\ell}\rangle = |\frac{1}{2}\rangle$  and  $|s_{z,r}\rangle = |\frac{1}{2}\rangle$ , then the resonance energy of the LPs in both left and right traps will increase by  $V_{\text{ex}}$ . At the same time the LPs in the two traps are coupled with coupling constant  $U$ . Thus it is evident that the evolution of the LP coherent state in the two traps depends on the spin of the electrons in both the QDs. Accounting for the leakage of polaritons from the cavity and solving the master-equation<sup>13</sup>, we obtain the LP coherent state evolution in the two traps:

$$\begin{aligned}\frac{d\alpha_{\ell}^s}{dt} &= \sqrt{\gamma_t} P(t) + U i \alpha_r^s + \left( -i(\delta_{\ell} + V_{\text{ex}} \langle \hat{\sigma}_{z,\ell} \rangle) - \frac{\gamma}{2} \right) \alpha_{\ell}^s, \\ \frac{d\alpha_r^s}{dt} &= \sqrt{\gamma_t} P(t) + U i \alpha_{\ell}^s + \left( -i(\delta_r + V_{\text{ex}} \langle \hat{\sigma}_{z,r} \rangle) - \frac{\gamma}{2} \right) \alpha_r^s, \\ s &= \frac{\langle \hat{\sigma}_{z,\ell} \rangle + \langle \hat{\sigma}_{z,r} \rangle}{2} = 1, 0, -1\end{aligned}\quad (10)$$

where,  $\alpha_{\ell(r)}^s$  is the coherent amplitude of  $\mathbf{k}_{\parallel} = \mathbf{0}$  LPs in left- $\ell$  (right- $r$ ) trap,  $\gamma_{t(b)}$  is the LP decay rate from the top(bottom) DBR mirror, and  $\gamma = \gamma_t + \gamma_b$ . The above expression has been derived under the approximation that  $\frac{g_{\ell(r)}^2}{\Delta_{\ell(r)}} \ll V_{\text{ex}}$ . Furthermore, the dipole coupling can virtually drive the evolution of the QD electron spin

state:

$$\left| \frac{1}{2} \right\rangle_{\ell(r)} \rightarrow \cos \tilde{\theta}_{\ell(r)}^s(t) \left| \frac{1}{2} \right\rangle_{\ell(r)} + \sin \tilde{\theta}_{\ell(r)}^s(t) \left| \frac{3}{2} \right\rangle_{\ell(r)} \quad (11)$$

where, the angle  $\tilde{\theta}_{\ell(r)}$  is given by:

$$\cos \tilde{\theta}_{\ell(r)}(t) = \frac{\Delta_{\ell(r)} - V_{\text{ex}} |\alpha_{\ell(r)}^s|^2}{\sqrt{((\Delta_{\ell(r)} - V_{\text{ex}} |\alpha_{\ell(r)}^s|^2)^2 + g_{\ell(r)}^2 |\alpha_{\ell(r)}^s|^2)}}, \quad (12)$$

$s = \frac{\langle \hat{\sigma}_{z,\ell} \rangle + \langle \hat{\sigma}_{z,r} \rangle}{2} = 1, 0, -1$ . Note that the angle  $\tilde{\theta}_{\ell(r)}(t)$  is a function of  $\alpha_{\ell(r)}^s$  and hence depends on the spin state of both the QD electrons. Since  $\Delta_{\ell(r)}$  is large and pumping power is small we find that  $1 > \cos \tilde{\theta}_{\ell(r)}(t) > 0.998$  (i.e., the probability for a real excitation of the trion level  $< 0.1\%$ ). If at time  $t = 0$ , the spin state is:  $|\Phi(t=0)\rangle = |\frac{1}{2}, \frac{1}{2}\rangle + |\frac{1}{2}, -\frac{1}{2}\rangle + |-\frac{1}{2}, \frac{1}{2}\rangle + |-\frac{1}{2}, -\frac{1}{2}\rangle$ , then, after the application of the pump pulse, the state will be:  $|\Phi(t)\rangle = e^{i\phi^1} |\frac{1}{2}, \frac{1}{2}, \alpha_{\ell}^1, \alpha_r^1\rangle + e^{i\phi^0} |\frac{1}{2}, -\frac{1}{2}, \alpha_{\ell}^0, \alpha_r^0\rangle + e^{i\phi^0} |-\frac{1}{2}, \frac{1}{2}, \alpha_{\ell}^0, \alpha_r^0\rangle + e^{i\phi^{-1}} |-\frac{1}{2}, -\frac{1}{2}, \alpha_{\ell}^{-1}, \alpha_r^{-1}\rangle$ . There are two processes contributing to the phase  $\phi^s$ :

1. The coherent states  $\alpha_{\ell}^s$  and  $\alpha_r^s$  follow a cyclic path in the phase space, conditional on the state of the two qubits (Eqn. 10). The resulting geometric phase depends on the area of these paths:

$$\phi_g^s = \Im \left( \int \alpha_{\ell}^s d\alpha_{\ell}^{s*} + \int \alpha_r^s d\alpha_r^{s*} \right) \quad (13)$$

It can be shown that the dynamic phase resulting from the evolution of the coherent states,  $\phi_d^s = -2\phi_g^s$  and hence the total phase still depends only on global geometric features<sup>50</sup>.

2. The evolution of the QD electron state (Eqn. 11,12) is analogous to the cyclic evolution of a spin- $\frac{1}{2}$  particle in a rotating magnetic field and the resulting Aharonov-Anandan phase acquired is<sup>51</sup>:

$$\begin{aligned}\phi_g^1 &= \int \frac{\omega}{2} (1 - \cos \tilde{\theta}_{\ell}^1(t)) dt + \int \frac{\omega}{2} (1 - \cos \tilde{\theta}_r^1(t)) dt, \\ \phi_g^0 &= \int \frac{\omega}{2} (1 - \cos \tilde{\theta}_{\ell}^0(t)) dt, \\ &= \int \frac{\omega}{2} (1 - \cos \tilde{\theta}_r^0(t)) dt, \\ \phi_g^{-1} &= 0.\end{aligned}\quad (14)$$

This evolution would also result in a dynamic phase, which must be removed by application of a second pulse in order to implement a purely geometric phase gate.

The Coulomb exchange interaction results in non-linearity in phases, so that  $\Theta = \phi^1 + \phi^{-1} - 2\phi^0 \neq 0$ . This non-linear phase  $\Theta$  leads to entanglement and for a controlled-z gate we must apply the pulse, such that,  $\Theta = (2n + 1)\pi$ .

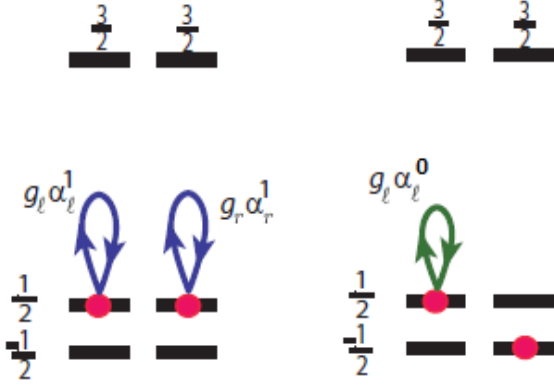


FIG. 5. Diagrammatic representation of the perturbative dipole coupling between the photonic part of the polaritons and the QD electron-trion transition. The coupling strength proportional to the amplitude of the LP coherent state, which in turn depends on the spin state of both electrons through Eqn. 10.

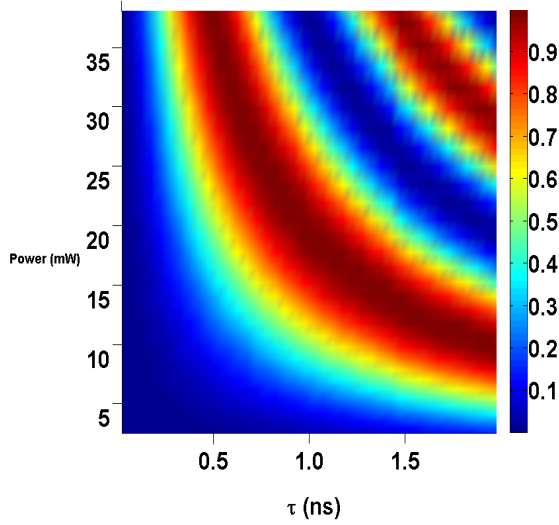


FIG. 6. Plot showing the dependence of two-qubit gate fidelity on peak pump power  $|P_0|^2 \hbar \omega$  and pulse width  $\tau$ . Note that the pump is far-red detuned ( $\delta$ ) from the  $\mathbf{k}_{\parallel} = \mathbf{0}$  LP resonance. Since the detuning is much larger than the cavity linewidth ( $\delta \gg \gamma$ ), the circulating power inside the cavity is small. For example for an input power of 30 mW, the circulating power inside the cavity for a detuning of  $\delta = 5$  meV, the peak photon number inside the cavity  $N = 36$  and  $P_c = \frac{N \hbar \omega c}{2L_c} = 0.8$  mW.

### A. Two-qubit Gate Fidelity

If  $\gamma = 0$ , then with proper pump parameters, it is possible to achieve the final state  $|\Phi_0(T)\rangle = -|\frac{1}{2}, \frac{1}{2}\rangle + |\frac{1}{2}, -\frac{1}{2}\rangle + |-\frac{1}{2}, \frac{1}{2}\rangle + |-\frac{1}{2}, -\frac{1}{2}\rangle$ . Nonetheless, in the pres-

ence of decoherence ( $\gamma \neq 0$ ), the qubit state is no longer a pure state and must be represented by a density matrix  $\rho$ . The evolution of the density matrix is described by the master-equation:  $\frac{d\rho}{dt} = -i[\hat{H}, \rho] + \sum_{k=\ell, r} \gamma a_k \rho a_k^\dagger - \frac{\gamma}{2} \{a_k^\dagger a_k, \rho\}$ <sup>13</sup>. By solving the master-equation it is easily shown that the coherence between the states  $|j_\ell, j_r\rangle$  and  $|k_\ell, k_r\rangle$  decays exponentially as  $\exp(-\frac{\gamma}{2}|\alpha_\ell^{s_1} - \alpha_\ell^{s_2}|^2 - \frac{\gamma}{2}|\alpha_r^{s_1} - \alpha_r^{s_2}|^2)$ , with  $j_i, k_i = \pm\frac{1}{2}$ ,  $s_1 = j_\ell + j_r$  and  $s_2 = k_\ell + k_r$ <sup>6,13</sup>. As a result, the fidelity of the gate operation  $F = \text{Tr}[\rho|\Phi_0\rangle\langle\Phi_0|\rho] < 1$ . The probability to excite the trion level is  $\sim 10^{-3}$  and thus the contribution to decoherence from spontaneous emission will be much smaller. Figure 6 plots the fidelity of the two-qubit geometric controlled-z gate described above for a Gaussian pump pulse  $P(t) = P_0 e^{-\frac{t^2}{\tau^2}}$ . The pump is red-detuned from the LP resonance by  $\delta_\ell = \delta_r = 5$  meV, so that  $\Delta_\ell = \Delta_r = 15$  meV. As we mentioned previously, if the trap radius  $R = 1 \mu\text{m}$  and distance between the two traps  $= 3.5 \mu\text{m}$ , then,  $V_{\text{ex}} = 2 \mu\text{eV}$  and  $U = 0.5$  meV. In this example we assume the cavity quality factor of  $Q = 76,000$ , so that the photon decay rate  $\gamma_p = 0.02$  meV. The lifetime of a QW exciton is  $\sim 1$  ns<sup>23</sup>, so that,  $\gamma_x = 4 \mu\text{eV}$  and the polariton decay rate  $\gamma = |t_0^2|\gamma_p + |r_0^2|\gamma_x = \frac{\gamma_p}{2} + \frac{\gamma_x}{2} = 0.012$  meV. The plot is characterized by alternating regions of high ( $\Theta = (2n+1)\pi$ ) and low ( $\Theta = 2n\pi$ ) fidelity. It is easy to show that,  $\Theta \propto P_0^2 \tau$ , which means that, if  $P_0$  increases then  $\tau$  must decrease in order to achieve the same fidelity. This feature is represented by the shape of the stripe pattern in Fig. 6. Note that, in this plot we have only considered the geometric contribution to the phase. The performance of the gate however depends on the total fidelity achieved after the application of the second pulse to cancel the dynamic phase.

In our parameter regime, the non-linear dynamic phase is negative while the total non-linear phase and geometric phase are positive ( $\Theta_g > |\Theta_d| > \Theta$ ). Thus, one can apply a second pulse, such that, the total phase acquired after its application cancels the dynamic phase of the first pulse ( $\Theta_{d, \text{pulse 1}} + \Theta_{\text{pulse 2}} = 0$ ). Consequently, the total phase after the two pulses has only a geometric component. Table I lists the pulse parameters, gate time and fidelity achievable for cavities with  $Q = 76,000$  and  $Q = 30,000$ . It also compares the gate times and fidelity for a purely geometric gate and a phase gate (i.e., in which the phase has both dynamic and geometric components). A parameter of interest in the Cooperativity factor and when the QD electron-trion transition is on resonance with the cavity mode  $C_0 = \frac{4g_{\ell(r)}^2}{\gamma_p \kappa} = \frac{3\lambda_0^3 Q}{4\pi^2 n^3 V}$ , where  $\gamma_p$  is the photon linewidth,  $\kappa$  is the spontaneous emission rate of the QD,  $\lambda_0$  is the cavity photon wavelength in vacuum,  $n$  is the refractive index of the cavity,  $Q$  is the cavity quality factor and  $V$  is the cavity mode volume. It represents the factor by which spontaneous emission is enhanced due to the cavity. At zero detuning, the cooperativity factor is enhanced by the cavity  $Q$ . However, when the QD electron-trion transition is

detuned by an amount  $\Delta(\gg \gamma)$  from the cavity, then the spontaneous emission into the cavity mode is suppressed by  $Q$ . The cooperativity factor is the figure of merit for a two-qubit gate based on dispersive interaction

with the cavity photon mode and for a high fidelity operation  $C_0 > 10^3$  is required<sup>1</sup>. Table I suggests that in our scheme, it is possible to achieve a high fidelity two-qubit operation with smaller cooperativity factors.

TABLE I. Two-qubit controlled- $z$  geometric and phase gate times ( $\tau_{\text{gate}}$ ) and fidelity ( $F$ ) for different cavity quality factors ( $Q$ ). The parameters used are  $V_{\text{ex}} = 2 \mu\text{eV}$ ,  $J = 0.5 \text{ meV}$  and  $g_{\ell,r} = 0.04 \text{ meV}$ . The LP resonance is 20 meV blue detuned from the QD electron-trion transition, so that,  $\Delta_{\ell,r} = (\delta_{\ell,r} - 20) \text{ meV}$ . The input pump pulse is assumed to have a Gaussian profile  $P = P_0 e^{-\frac{t^2}{\tau^2}}$ .

	Q	$\gamma_{\text{p}}$ (meV)	$\gamma$ (meV)	$C_0$	$\delta$ (meV)	Peak power $= \hbar\omega P_0^2$ (W)	$\tau$ (ns)	$\tau_{\text{gate}}$ (ns)	F (%)
Geometric Phase Gate									
Pulse 1	76,000	0.02	0.012	$\sim 187$	10	0.47	2.36	15.96	99.6
Pulse 2					7	0.47	1.63		
Phase Gate									
Pulse 1	76,000	0.02	0.012	$\sim 187$	10	0.47	9.32	37.28	99.45
Geometric Phase Gate									
Pulse 1	30,000	0.05	0.027	$\sim 73$	12	0.47	4.2	23.8	99.4
Pulse 2					6	0.47	1.75		
Phase Gate									
Pulse 1	30,000	0.05	0.027	$\sim 73$	12	0.47	16.88	67.52	99.1

## VII. QUANTUM NON-DEMOLITION MEASUREMENT

Next we will describe a scheme to achieve a fast, high fidelity, single-shot, QND measurement of the spin state of the QD electron. In section I we discussed the importance of eliminating any back-action during the read-out process. The inherent spectral separation between the QD and QW excitations ensures that a probe pulse close to the QW LP resonance does not excite the QD single electron to trion or p-shell states. This eliminates the read-out backaction in the form of a spin-flip transition via excited states. We propose to use the QND read-out mechanism introduced in ref. 14. We will briefly describe the principle of the readout scheme. Figure 7 illustrates the setup proposed for performing a QND measurement operation. A horizontally (H) polarized probe laser, slightly detuned from the LP resonance ( $\delta$ ), is incident normally over the QD whose electron spin is to be measured. Following the arguments in section III, the nearest neighbor traps must also be appropriately pumped to minimize its coupling with the target trap (T). In the following analysis we will assume that LPs are only injected in the trap (T) and the small error introduced due to coupling with neighboring traps will be quantified in section VIII.B

The H-polarized probe beam will excite both  $J = 1$  and  $J = -1$  LPs in the trap T. As described by Eqn. 6, the degeneracy between the  $J = 1$  and  $J = -1$  LPs is lifted due to Coulomb exchange interaction with the QD electron spin qubit. The resonance energy of the LPs with

$J = 1(-1)$  experience a red or blue (blue or red) shift if the spin state of QD electron is  $|\frac{1}{2}\rangle$  or  $|\frac{-1}{2}\rangle$ . Consequently, the  $J = 1$  and  $J = -1$  LPs evolve with different phases and amplitudes. This is manifested by the introduction of a small vertically (V) polarized component in the light reflected from the cavity. The reflected light is elliptically polarized with its axis tilted by an angle  $\propto \pm V_{\text{ex}}$  (depending on whether  $|s_z\rangle = |\pm\frac{1}{2}\rangle$ ). As explained in section V, the Faraday magnetic field also lifts the degeneracy between the  $J = 1$  and  $J = -1$  LPs ( $2V \sim 100 \mu\text{eV}$ ), introducing a non-zero baseline signal<sup>6,16</sup>. The major difference between the setup in ref. 14 and our scheme in the current work is that we now suggest the use of etched polariton traps to increase the exchange interaction between a QD electron and a polariton. Whereas in a planar cavity with no traps we estimated  $V_{\text{ex}} \sim 0.2 \mu\text{eV}$ , with traps of radius  $1 \mu\text{m}$ , we estimate  $V_{\text{ex}} \sim 2 \mu\text{eV}$ . Using this value, we redid the numerical calculations in ref. 14, and we find that the measurement can now be performed an order of magnitude faster. Table II shows the results of these calculations. Reference 14 also describes various possible sources of readout errors, namely: shot-noise error, phonon-assisted spin-flip scattering and radiative recombination of QD electron with QW holes. However, in the setup proposed here, there is an additional source of crosstalk error due to polariton tunneling between neighboring traps. In the next section we describe in detail the procedure to estimate this error

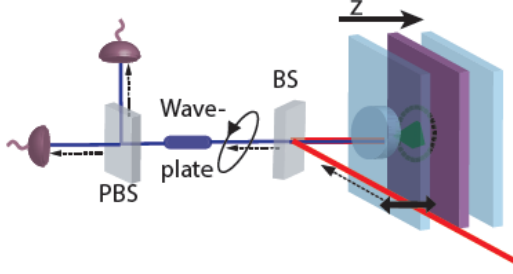


FIG. 7. Illustration of the QND measurement setup. The dotted line shows the trap region in the QW in which the LPs are excited.

### A. Crosstalk due to tunnel coupling with neighboring traps

In section III we outlined a scheme to minimize the coupling of LPs in neighboring traps. Despite this, some LPs are injected in the neighboring traps. These LP modes interact with the neighboring electron spin qubits, leading to decoherence. Consider the setup described in section III (Fig. 2(c)). Suppose, the spin state of the electrons trapped in the QDs over the target trap is  $|\frac{1}{2}\rangle_T$  and spin state in the neighboring traps is the maximally entangled state  $|\psi\rangle = \frac{1}{\sqrt{2}}(|\frac{1}{2}_1, \frac{1}{2}_2, \frac{1}{2}_3 \dots\rangle + |-\frac{1}{2}_1, -\frac{1}{2}_2, -\frac{1}{2}_3 \dots\rangle)$ . We choose this state for the neighboring qubits as it will experience maximum decoherence. After the application of the measurement pulses  $F$  and  $F_T$ , the spin state of the target qubit will be projected on to the state  $|\frac{1}{2}\rangle_T$ . But the state of the neighboring qubits will be a mixed state represented by the density matrix  $\rho_f$ . The error introduced in the states of neighboring qubits during a measurement of the target qubit is:  $P_e^c = 1 - F$ , where  $F = \text{Tr}[\sqrt{\rho_f}|\psi\rangle\langle\psi|\sqrt{\rho_f}]$  is the fidelity. In the example presented in table II, if a measurement is made in a single-sided (symmetric two-sided) cavity for  $\tau_{\text{meas}} = 660(750)$  ps with  $F_T = 41.1(70.8) 1/\sqrt{\text{ps}}$  at  $\delta = 0.3$  meV, then the probability of error introduced in the neighboring spin state is  $P_e^c \sim 0.002(0.004)\%$ . Thus, it is desirable to make a measurement at  $\delta = 0.3$  meV and hence for  $V = 50 \mu\text{eV}$  ( $\Rightarrow V \ll \delta$ ), the measurement time and fidelity is not affected by the Faraday magnetic field<sup>16</sup>.

## VIII. SINGLE-QUBIT OPERATION

Finally, in order to achieve universal quantum computation, we must be able to implement rotations of a single spin-qubit on the Bloch sphere. From the analysis in section III, it is evident that by using an off-resonant pulse, it is possible to excite LPs in a single trap. Suppose the initial state of the electron-spin localized in the QD above the target trap is  $|\psi(t=0)\rangle = \frac{1}{\sqrt{2}}(|\frac{1}{2}\rangle + |-\frac{1}{2}\rangle)$ .

TABLE II. Required measurement times  $\tau_{\text{meas}}$  and average LP number  $\langle N \rangle$ , required to achieve the shot noise error  $P_e^{\text{sn}} = 0.1\%$ . The total LP decay rate is taken as  $\gamma = 0.027$  meV corresponding to a cavity with  $Q=30,000$ . The table also lists the probability of error introduced in the neighboring qubits ( $P_e^t$ ) when they are in their maximally entangled state.

$V_s = 0$	$\delta(\text{meV})$	Phase Measurement		
		$\tau_{\text{meas}}$	$\langle N \rangle$	$P_e^t$
Single-Sided Cavity	0.3	660 ps	525	0.002%
	0.1	360 ps	90	0.1%
Symmetric Two-Sided Cavity	0.3	750 ps	750	0.004%
	0.1	360 ps	170	0.2%
$V_s = 0.15$ meV	$\delta(\text{meV})$	Intensity Measurement		
		$\tau_{\text{meas}}$	$\langle N \rangle$	$P_e^t$
Single-Sided Cavity	0.15	360 ps	25	0.03%
$V_s = 0.15$ meV	$\delta(\text{meV})$	Phase Measurement		
		$\tau_{\text{meas}}$	$\langle N \rangle$	$P_e^t$
Symmetric Two-Sided Cavity	0.14	360 ps	160	0.2%

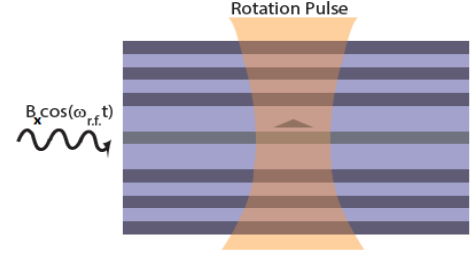


FIG. 8. The figure shows an in-plane r.f. magnetic field of small strength. In the absence of any optical pulse, the in-plane field is far-red detuned from the Zeeman splitting of the QD electron spin state. When an optical pulse is applied to excite LPs with  $\langle a_{-1}^\dagger a_{-1} \rangle = N$  such that  $E_z - V_{\text{ex}}N$ , the spin qubit rotates about the x-(or y-) axis.

Following the arguments presented in section VI, it is easy to see that after a time  $t$  the state of the system will be  $|\psi(t)\rangle = \frac{1}{\sqrt{2}}(|\frac{1}{2}, \alpha_{\frac{1}{2}}\rangle + e^{i\frac{\theta_z}{2}}|-\frac{1}{2}, \alpha_{-\frac{1}{2}}\rangle)$ . Thus, under proper pulse parameters, it is possible to achieve a single-qubit rotation about the  $z$  axis. However, a similar rotation about the  $x$  (or  $y$ ) axis would require a control Hamiltonian of the form  $\hat{H}_{x(y)} \propto \sigma_{x(y)}$ . This Hamiltonian cannot be achieved with QW polaritons because the quantum confinement effect restricts the polarization of the 2D-polaritons along the growth ( $z$ ) axis<sup>52</sup>. Thus, in order to achieve arbitrary qubit rotations we propose to use an external in-plane r.f. magnetic field (of magnitude  $B_x$  and frequency  $\omega_{\text{r.f.}}$ ) as shown in Fig. 8. The vertical magnetic field  $B_0$  leads to a Zeeman splitting of  $E_z = g\mu_B B_0$ , where  $g$  is the electron  $g$ -factor in the QD and  $\mu_B$  is the Bohr magneton. The amplitude of the in-plane magnetic field  $B_x$  is such that  $E_z > \omega_{\text{r.f.}}$  and  $g\mu_B B_x \ll E_z - \omega_{\text{r.f.}}$ . This ensures that, in the absence of an optical pump the in-plane magnetic field does

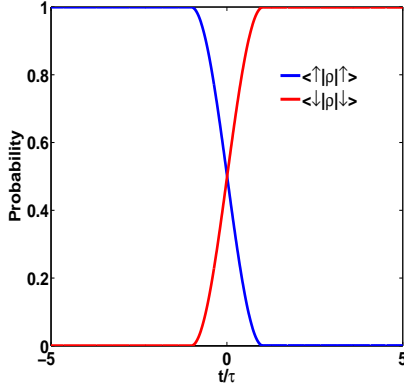


FIG. 9. Plot of probabilities  $\langle \frac{1}{2} | \rho | \frac{1}{2} \rangle^2$  and  $\langle -\frac{1}{2} | \rho | -\frac{1}{2} \rangle^2$  as a function of time during the application of a  $\pi$ -rotation pulse.

not rotate the spin qubits. A  $\sigma_-$  pump pulse (red detuned from the LP resonance by  $\delta$ ) is applied over the QD to excite  $J = -1$  LPs in the trap directly below the it. The exchange interaction between the QD electron and  $J = -1$  LPs is represented by the Hamiltonian  $\hat{H} = -V_{\text{ex}} a_{-1}^\dagger a_{-1} \hat{\sigma}_z$ . The key idea is to realize that this interaction leads to the modulation of the Zeeman energy of the QD electron spin by an amount  $\propto -V_{\text{ex}} a_{-1}^\dagger a_{-1}$ . Thus when  $E_z - V_{\text{ex}} \langle a_{-1}^\dagger a_{-1} \rangle = \omega_{\text{r.f.}}$ , the in-plane magnetic field rotates the spin along the  $x$  axis. The angle by which the spin rotates is determined by length of the pump pulse. The rotation axis is determined by the arrival time of the pump pulse. For example, if the pump pulse arrives at time  $\tau_{\text{arriv}}$  so that the in-plane magnetic field is in-phase ( $180^\circ$  out-of-phase) then the qubit rotates about the  $x(y)$  axis. Note that, due to the dynamics described in section VI, the qubit will also be rotated (at a rate  $\propto NV_{\text{ex}}$ ) about the  $z$ -axis, but the parameters can be easily chosen such that during a  $(2n+1)\pi$  rotation about the  $x$  axis, the qubit rotates by  $2m\pi$  about the  $z$ -axis. Suppose that at  $t = 0$ , the spin state of the qubit is  $|\frac{1}{2}\rangle$ . The rotation pulse  $F_{\text{T}}$  is red-detuned from the LP by  $\sim 6$  meV and in its pulse shape is given by:

$$\begin{aligned} F_{\text{T}} &= F_0 e^{-\frac{|t+\tau|^2}{\tau_{\text{F}}^2}} \quad \forall \quad t < -\tau, \\ &= F_0 \quad \forall \quad -\tau \leq 0 \leq \tau, \\ &= F_0 e^{-\frac{|t-\tau|^2}{\tau_{\text{F}}^2}} \quad \forall \quad t > \tau, \end{aligned} \quad (15)$$

with  $F_0 = 769.8 (\sqrt{\text{meV}})^{-1}$ ,  $\tau = 200$  ps and  $\tau_{\text{F}} = 5$  ps. The value of  $F_0$  is chosen so that in a symmetric two-sided

cavity with  $\gamma = 0.027$  meV, the average number of LPs at equilibrium  $\langle a_{-1}^\dagger a_{-1} \rangle = N = 500$  and thus,  $V_{\text{ex}} N = 1$  meV (for  $V_{\text{ex}} = 2 \mu\text{eV}$ ). The in-plane magnetic field is of magnitude  $B_x = 0.023$  mT and frequency such that  $E_z - \omega_{\text{r.f.}} = 1$  meV. This results in the  $\pi$  rotation of the spin-qubit within  $\sim 420$  ps. Figure 9 plots  $\langle \frac{1}{2} | \rho(t) | \frac{1}{2} \rangle^2$  and  $\langle -\frac{1}{2} | \rho(t) | -\frac{1}{2} \rangle^2$  during the application of a  $\pi$ -rotation pulse. The major source of decoherence in this scheme is the loss of polaritons from the cavity. Suppose the initial state of the electron-spin qubit is  $|\psi(t=0)\rangle = \frac{|\frac{1}{2}\rangle + |-\frac{1}{2}\rangle}{\sqrt{2}}$ . If we now apply a pulse to rotate the qubit by  $\pi$  about the  $x$ -axis, the final state should remain the same i.e.,  $|\psi(T)\rangle = |\psi(0)\rangle$ . But due to decoherence the final state is actually a mixed state, represented by the density matrix  $\rho$ . The success of the gate is determined by the fidelity  $F$  (evaluated like in section VI.A). For the parameters used in Fig. 9, the fidelity for a single qubit  $\pi$  rotation is 99.8%. Another approach to evaluate the decoherence is to note that the injected LPs are in a coherent state and thus there are quantum fluctuations in the number of LPs, i.e.,  $\Delta(N) = \sqrt{N}$ , where  $N = \langle a_{-1}^\dagger a_{-1} \rangle$ . These fluctuations lead to decoherence of the qubit and can be evaluated as outlined in ref. 53. This results in an identical estimate for error probability = 0.2%.

## IX. CONCLUSION

To summarize, table III lists the theoretical gates times and fidelities that can be achieved in QD spin qubits using the proposed technique of indirect optical control mediated by QW LPs. The table also compares its performance with that of the existing optical schemes. The improvement in the two-qubit gate scheme is evident from the decrease in the cooperativity  $C_0$  (by a factor  $\sim 100$  for  $F = 99.4\%$ ) required to achieve a high fidelity operation. In our scheme it would also be possible to achieve a single-qubit rotation in Faraday geometry within  $\sim 420$  ps and a fidelity of 99.8%. An improvement in the QND measurement time of a factor of 30 is achieved, but more importantly, the probability of error is reduced by a factor of  $\sim 200$ . In conclusion, these results predict that it could be possible to realize a scalable architecture for quantum computation based on semiconductor QD spins using the QW polariton resonance, and which fulfills the requirements for fault-tolerant operation using the surface code.

## X. REFERENCES

TABLE III. Comparison of the theoretical gates times, fidelity and the required cooperativity ( $C$ ) (for two-qubit operation) that can be achieved with QD electron qubits using the proposed technique of indirect optical control mediated by QW LPs with the existing optical schemes.

	Current Optical Schemes		Proposed Scheme with QW LPs	
	Gate Time	Fidelity	Gate Time	Fidelity
Two-qubit gate	100 ns <sup>6</sup>	99.9% <sup>6</sup>	24 ns	99.4%
C	10 <sup>3</sup>		20	
Single-qubit operation	Not possible in Faraday geometry, in QDs using optical pulses and no local wiring (but possible in gate defined QDs).		420 ps	99.8%
QND measurement	20 ns <sup>11,54</sup>	95% <sup>11,54</sup>	660 ps	99.97%
			Single-sided cavity	

- <sup>1</sup> N. C. Jones, R. Van Meter, A. G. Fowler, P. L. McMahon, J. Kim, T. D. Ladd and Y. Yamamoto, *Phys. Rev. X* **2**, 031007 (2012)
- <sup>2</sup> C. Schneider, M. Strauß, T. Sunner, A. Huggenberger, D. Wiener, S. Reitzenstein, M. Kamp, S. Höfling and A. Forchel, *Appl. Phys. Lett.* **92**, 183101 (2008)
- <sup>3</sup> K. De.Greve, D. Press, P. L. McMahon and Y. Yamamoto, *Rep. Prog. Phys.* **76**, 092501 (2013)
- <sup>4</sup> D. Press, T. D. Ladd, B. Zhang and Y. Yamamoto, *Nature* **456** 218 (2008)
- <sup>5</sup> A. Imamoglu, D. D. Awschalom, G. Burkard, D. P. DiVincenzo, D. Loss, M. Sherwin, and A. Small, *Phys. Rev. Lett.* **83**, 4204 (1999)
- <sup>6</sup> T. D. Ladd and Y. Yamamoto, *Phys. Rev. B* **84**, 235307 (2011)
- <sup>7</sup> K. Ujihara, *Jpn. J. Appl. Phys.* **33** 1059 (1994)
- <sup>8</sup> M. Osuge and K. Ujihara, *J. Appl. Phys.* **76**, 2588 (1994)
- <sup>9</sup> G. Björk, H. Heitmann, and Y. Yamamoto, *Phys. Rev. A* **47**, 4451 (1993)
- <sup>10</sup> M. Atatüre, J. Dreiser, A. Badolato, and A. Imamoglu, *Nature Physics* **3**, 101 (2007)
- <sup>11</sup> A. Delteil, W. B. Gao, P. Fallahi, J. Miguel-Sanchez, and A. Imamoglu, *Phys. Rev. Lett.* **112**, 116802 (2014)
- <sup>12</sup> A. N. Vamivakas, C. -Y. Lu, C. Matthiesen, Y. Zhao, S. Fält, A. Badolato, and M. Atatüre, *Nature* **467**, 297 (2010)
- <sup>13</sup> S. Puri, N. Y. Kim and Y. Yamamoto, *Phys. Rev. B* **85**, 241403(R) (2012)
- <sup>14</sup> S. Puri, P. L. McMahon, and Y. Yamamoto arXiv:1310.4873
- <sup>15</sup> P. Lugin, D. Sarchi, and V. Savona *Phys. Stat. Sol. (c)* **3**, 2428 (2006)
- <sup>16</sup> See Supplemental Material
- <sup>17</sup> O. El. Daïf, A. Baas, T. Guillet, J. -P. Brantut, R. I. Kaitouni, J. L. Staehli, F. Morier-Genoud, and B. Deveaud, *Appl. Phys. Lett.* **88**, 061105 (2006)
- <sup>18</sup> A. Muller, C.-K. Shih, J. Ahn, D. Lu, D. Gazula, and D. G. Deppe, *Appl. Phys. Lett.* **88**, 031107 (2006)
- <sup>19</sup> C. Weisbuch, M. Nishioka, A. Ishikawa, and Y. Arakawa, *Phys. Rev. B* **69**, 3314 (1992)
- <sup>20</sup> H. Deng, G. Weihs, D. W. Snoke, J. Bloch, and Y. Yamamoto, *Proc. Natl. Acad. Sci. U.S.A.* **100**, 15318 (2003)
- <sup>21</sup> M. I. Dyakonov, *Spin Physics in Semiconductors* Springer series in solid-state sciences (Springer-Verlag Berlin Heidelberg 2008)
- <sup>22</sup> I. A. Shelykh, A. V. Kavokin, and G. Malpuech, *Phys. Status Solidi (b)* **242**, 2271 (2005)
- <sup>23</sup> H. Deng, H. Haug, and Y. Yamamoto, *Rev. Mod. Phys.* **82**, 1489 (2010)
- <sup>24</sup> D. Sarchi, I. Carusotto, M. Wouters, and V. Savona, *Phys. Rev. B* **77**, 125324 (2008)
- <sup>25</sup> C. Piermarocchi, P. Chen, L. J. Sham, and D. G. Steel, *Phys. Rev. Lett.* **89** 167402 (2002)
- <sup>26</sup> G. F. Quinteiro, J. Fernandez-Rossier, and C. Piermarocchi, *Phys. Rev. Lett.* **97**, 097401 (2006)
- <sup>27</sup> B. Urbaszek, R. J. Warburton, K. Karrai, B. D. Gerardot, P. M. Petroff, and J. M. Garcia, *Phys. Rev. Lett.* **90**, 247403 (2003)
- <sup>28</sup> J. J. Hopfield, *Phys. Rev.*, **112** 1555 (1958)
- <sup>29</sup> L. C. Andreani, G. Panzarini, and J.-M. Gérard *Phys. Rev. B* **60**, 13276 (1999)
- <sup>30</sup> J. P. Reithmaier, G. Sek, A. Löffler, C. Hofmann, S. Kuhn, S. Reitzenstein, L. V. Keldysh, V. D. Kulakovskii, T. L. Reinecke, and A. Forchel, *Nature* **432**, 197 (2004)
- <sup>31</sup> R. Hanson, L. P. Kouwenhoven, J. R. Petta, S. Tarucha, and L. M. K. Vandersypen, *Rev. Mod. Phys.* **79**, 1217 (2007)
- <sup>32</sup> A. V. Khaetskii and Y. V. Nazarov, *Phys. Rev. B* **64**, 125316 (2001)
- <sup>33</sup> V. N. Golovach, A. Khaetskii, and D. Loss, *Phys. Rev. Lett.* **93**, 016601 (2004)
- <sup>34</sup> K. De Greve, P. L. McMahon, D. Press, T. D. Ladd, D. Bisping, C. Schneider, M. Kamp, L. Worschech, S. Höfling, A. Forchel, and Y. Yamamoto, *Nature Phys.* **7**, 872 (2011)
- <sup>35</sup> X. Xu, B. Sun, P. R. Berman, D. G. Steel, A. S. Bracker, D. Gammon, and L. J. Sham, *Nature Phys.* **4**, 692 (2009)
- <sup>36</sup> D. Press, K. De. Greve, P. McMahon, T. D. Ladd, B. Friess, C. Schneider, M. Kamp, S. Höfling, A. Forchel and Y. Yamamoto, *Nature Photon.* **4**, 367 (2010)
- <sup>37</sup> A. Rahimi-Iman, C. Schneider, J. Fischer, S. Holzinger, M. Amthor, S. Höfling, S. Reitzenstein, L. Worschech, M. Kamp, and A. Forchel, *Phys. Rev. B* **84**, 165325 (2011)
- <sup>38</sup> A. Armitage, T. A. Fisher, M. S. Skolnick, D. M. Whitaker, P. Kinsler, and J. S. Roberts, *Phys. Rev. B* **55**, 16395

- (1997)
- <sup>39</sup> T. A. Fisher, A. M. Afshar, M. S. Skolnick, D. M. Whitaker, and J. S. Roberts, *Phys. Rev. B* **53**, R10 469 (1996)
- <sup>40</sup> R. Kotlyar, T. L. Reinecke, M. Bayer, and A. Forchel, *Phys. Rev. B* **63**, 085310 (2001)
- <sup>41</sup> L. Klotkowski, M. D. Martín, A. Amo, L. Viña, I. A. Shelykh, M. M. Glazov, G. Malpuech, A. V. Kavokin, and R. André, *Solid. State Commun.* **139**, 511 (2006)
- <sup>42</sup> G. Roumpos, C. W. Lai, T. C. H. Liew, Y. G. Rubo, A. V. Kavokin, and Y. Yamamoto, *Phys. Rev. B* **79** 195310 (2009)
- <sup>43</sup> F. Wilczek and A. Shapere, *Geometric phases in physics* *World Scientific, Singapore*, 1990
- <sup>44</sup> M. V. Berry, *Proc. R. Soc. Lond. A* **392**, 45 (1984)
- <sup>45</sup> Y. Aharonov and J. Anandan, *Phys. Rev. Lett.* **58**, 1593 (1987)
- <sup>46</sup> S.-L. Zhu and P. Zanardi, *Phys. Rev. A* **72**, 020301(R) (2005)
- <sup>47</sup> J. A. Jones, V. Vedral, A. Ekert, and G. Castagnoli, *Nature* **403** 869 (2000)
- <sup>48</sup> P. J. Leek, J. M. Fink, A. Blais, R. Bianchetti, M. Göppl, J. M. Gambetta, D. I. Schuster, L. Frunzio, R. J. Schoelkopf, and A. Wallraff, *Science* **318**, 1889 (2007)
- <sup>49</sup> X. B. Wang and K. Matsumoto, *Phys. Rev. Lett.*, **87** 097901 (2001)
- <sup>50</sup> S.-B. Zheng, *Phys. Rev. A* **70**, 052320 (2004)
- <sup>51</sup> S.-L. Zhu, Z. D. Wang, and Y.-D. Zhang, *Phys. Rev. B* **61**, 1142 (2000)
- <sup>52</sup> R. Winkler, D. Culcer, S. J. Papadakis, B. Habib, and M. Shayegan, *Semicond. Sci. Technol.* **23**, 114017 (2008)
- <sup>53</sup> D. I. Schuster, A. Wallraff, A. Blais, L. Frunzio, R.-S. Huang, J. Majer, S. M. Girvin, and R. J. Schoelkopf, *Phys. Rev. Lett.* **94**, 123602 (2005)
- <sup>54</sup> O. Gazzano, S. Michaelis de Vasconcellos, C. Arnold, A. Nowak, E. Galopin, I. Sagnes, L. Lanco, A. Lemaître, and P. Senellart, *Nat. Commun.* **4**, 1425 (2013).

## I. POLARITON TUNNEL COUPLING BETWEEN NEIGHBORING TRAPS

In this section we outline the method used to estimate the tunnel coupling constant ( $J$ ) between neighboring traps. Our method is motivated from the analysis in ref. 1. The main paper discussed how the local modulation of the cavity length created traps for polaritons. In order to estimate  $U$ , we model the traps as square potentials of depth  $\sim 7$  meV and sides of length  $2R$ . If the normal mode splitting ( $2\hbar\Omega_R$ ) between the upper polaritons (UPs) and lower polaritons (LPs) is larger than the coupling constant  $U$ , then the LPs at  $\mathbf{k}_{\parallel} = \mathbf{0}$  can be treated as quasi-particles of mass  $m_{LP}$ . Typically,  $2\hbar\Omega_R \sim 3 - 4$  meV and when the cavity photons are resonant with the quantum well (QW) excitons at  $\mathbf{k}_{\parallel} = \mathbf{0}$ , then  $m_{LP} \sim 4 \times 10^{-5} m_0$  ( $m_0$  is the mass of free electron). We can numerically evaluate the ground-state ( $E_{gs}$ ) and first excited-state ( $E_{es}$ ) energies of a LP (of mass  $m_{LP}$ ) in coupled square potential wells (each of depth 7 meV) by solving the time-independent Schrödinger equation:

$$\left( -\frac{\hbar^2 \nabla^2}{2m_{LP}} + U(x, y) \right) \Psi(x, y) = 0, \quad (16)$$

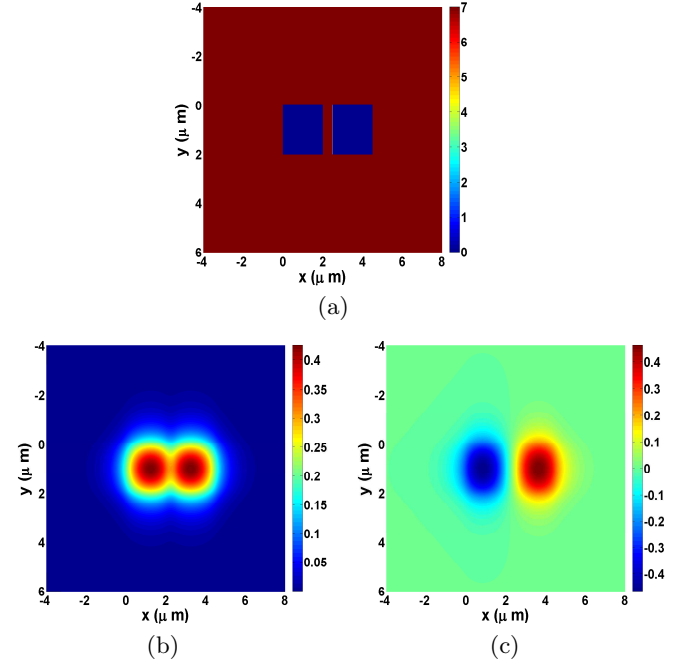


FIG. 10. (a) Illustration of the coupled LP traps, modeled as two square potential wells of depth 7 meV with sides of length  $2R$  ( $= 2 \mu\text{m}$ ) and separated by  $D$  ( $= 0.5 \mu\text{m}$ ). (b) and (c) Normalized ground state and excited state wavefunction of the LP in the coupled traps.

with the coupled square potential illustrated in Fig. 1(a) and given by:

$$\begin{aligned} U(x, y) &= 0, \quad 0 < x < 2R \quad \& \quad 0 < y < 2R \\ &= 0, \quad 2R + D < x < 4R + D \quad \& \quad 0 < y < 2R \\ &= 7 \text{ meV, everywhere else} \end{aligned} \quad (17)$$

Finally, the linear tunnel coupling strength is estimated as:

$$U = \frac{1}{2}(E_{es} - E_{gs}) \quad (18)$$

Fig. 1(b,c) show the ground state and excited state wavefunctions for  $D=0.5 \mu\text{m}$  and  $R = 1 \mu\text{m}$ . For these parameters and using Eqn. 18, we estimate  $U \sim 0.5$  meV.

## II. CAVITY MODE VOLUME

The mode volume of the cavity is calculated by first decoupling the field along the growth ( $z$ -axis) and in the cavity plane. This approximation is valid because of strong confinement of the photon modes along the growth direction. The mode volume then becomes  $V = AL$ , where  $A$  is the mode area and  $L$  is the mode length of the vertical cavity. The in-plane mode in a single trap can be calculated following the procedure in section I of the supplement and is approximated by the Gaussian

$\psi_{\parallel} = A_0 e^{-\frac{r^2}{a^2}}$ , where  $a = 1.2 \mu\text{m}$ . The effective cavity length  $L_c$  is a few wavelengths longer than the cavity length  $\lambda$ , due to the penetration of the cavity field into the DBR<sup>3</sup>:

$$L_c = \lambda + L_{\text{DBR}},$$

$$L_{\text{DBR}} = \frac{\lambda}{2} \frac{n_1 n_2}{n_c |n_1 - n_2|},$$

where  $n_1, n_2(n_c)$  are the refractive index for the materials of the DBR (cavity). For a GaAs/AlGaAs DBR mirrors and GaAs cavity,  $n_1 = 3$ ,  $n_2 = n_c = 3.6$ . The mode profile along the growth direction will be  $\psi_{\perp} = B_0 \sin\left(\frac{\pi z}{L_c}\right)$ .

Thus, the mode area and mode length are<sup>4</sup>:

$$A = \frac{\int_0^{\infty} |\psi_{\parallel}|^2 d^2 \mathbf{r}}{|\psi_{\parallel}|_{\text{max}}^2}, \quad L = \frac{\int_0^{\infty} |\psi_{\perp}|^2 dz}{|\psi_{\perp}|_{\text{max}}^2}$$

$$\Rightarrow A = \frac{\pi a^2}{2}, \quad L = \frac{L_c}{2} \quad (19)$$

Thus, the mode volume in the  $\lambda(=910 \text{ nm})$  cavity is  $V = 0.5 \mu\text{m}^3$ .

### III. EFFECT OF EXTERNAL FARADAY MAGNETIC FIELD ON HOPFIELD COEFFICIENTS

If the the  $J = 1$  ( $J = -1$ ) excitons are red(blue) detuned from the cavity photon by  $V = 50 \mu\text{eV}$  and if the Vacuum Rabi splitting is  $2\Omega_R = 3 \text{ meV}$ , then the excitonic and photonic fraction in the  $J = 1$  ( $J = -1$ ) LPs is:

$$|r_0|^2 = \frac{1}{2} \left( 1 \pm \frac{V}{\sqrt{V^2 + 4\Omega_R^2}} \right)$$

$$|t_0|^2 = \frac{1}{2} \left( 1 \mp \frac{V}{\sqrt{V^2 + 4\Omega_R^2}} \right) \quad (20)$$

Thus the excitonic, photonic fraction in the  $J = 1$  ( $J = -1$ ) LP is  $|r_0|^2, |t_0|^2 = 0.5083, 0.4957(0.9833, 0.4957)$  respectively.

### IV. DERIVATION OF RATE EQUATIONS FOR THE COHERENT POLARITON AMPLITUDE

In this section we will outline the procedure used to derive rate equations for the coherent polariton amplitude in the main paper (For example, Eqns. 1,2,10). In particular we will drive the Eqn. 1 of the main paper and the remaining equations can be derived in the same way. The Hamiltonian for the LPs in the target and nearest-neighbor traps (section III of the main paper) in

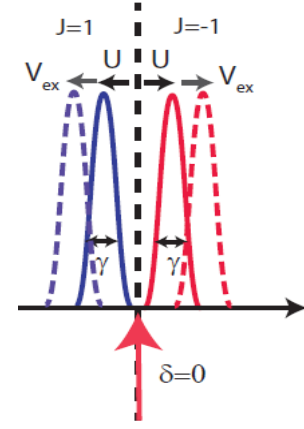


FIG. 11. A cartoon diagram showing the  $J = 1$  (blue) and  $J = -1$  (red) LP energy with respect to the probe detuning (horizontal axis). The solid lines represent the Lorentzian lineshape of the  $J = 1$  and  $J = -1$  LPs with width  $\gamma$  in the absence of QD electron. The dashed lines represent the shifted lineshapes when the QD spin state is  $\frac{1}{2}$

the rotating wave approximation is:

$$\hat{H} = \delta a_T^\dagger a_T + \sum_{i=1}^4 \delta a_i^\dagger a_i + U \sum_{i=1}^4 (a_T^\dagger a_i + a_i^\dagger a_T)$$

$$- i\sqrt{\gamma_t} F_T (a_T - a_T^\dagger) - i\sqrt{\gamma_t} F \sum_{i=1}^4 (a_i - a_i^\dagger) \quad (21)$$

We now describe the system with a density matrix  $\rho$ , which evolves according to the Lindbladian-master equation<sup>2</sup>:

$$\frac{d\rho}{dt} = -i[H, \rho] + \gamma p \rho p^\dagger - \frac{\gamma}{2} \{p^\dagger p, \rho\}. \quad (22)$$

Thus, one can derive the rate equation of coherent field amplitudes  $\alpha_T = \langle a_T \rangle$  ( $\alpha_i = \langle a_i \rangle$ ) as:

$$\frac{d\langle a_{T1,\dots,4} \rangle}{dt} = \text{Tr} \left[ \frac{d\rho}{dt} a_{T1,\dots,4} \right]$$

$$\Rightarrow$$

$$\frac{d\alpha_T}{dt} = \sqrt{\gamma_t} F_T - \left( i\delta + \frac{\gamma}{2} \right) \alpha_T - iU \sum_{i=1}^4 \alpha_i,$$

$$\frac{d\alpha_i}{dt} = \sqrt{\gamma_t} F - \left( i\delta + \frac{\gamma}{2} \right) \alpha_i - iU \alpha_T \quad (23)$$

### V. EFFECT OF FARADAY MAGNETIC FIELD ON QND MEASUREMENT SIGNAL

Next, we will briefly describe the effect of the external magnetic field, on the measurement signal operations. For the sake of simplicity we will assume  $V_s = 0$ , however the same analysis will hold when  $V_s \neq 0$ . As explained in

section, there will be a small anisotropy in the exchange energy. For example for a magnetic field  $B_0 = 2$  T, the fraction of the excitonic part ( $|r|_0^2$ ) in the LP will increase (decrease) by  $\sim 2\%$  (assuming a vacuum Rabi splitting of 3 meV at  $B_0 = 2$  T). For the example presented in the paper the exchange energy with the  $J = 1$  ( $J = -1$ ) LPs will be  $V_{\text{ex},1(-1)} = 0.2167(0.1933)$   $\mu\text{eV}$ . Thus, the Hamiltonian of the system in the rotating wave approximation is:

$$\begin{aligned}\hat{H} &= (\delta - V)a_1^\dagger a_1 + (\delta + V)a_{-1}^\dagger a_{-1} \\ &\quad - V_{\text{ex},1}\hat{\sigma}_z a_1^\dagger a_1 + V_{\text{ex},-1}\hat{\sigma}_z a_{-1}^\dagger a_{-1} \\ &\quad + i\sqrt{\gamma_t}f_0(a_H^\dagger - a_H), \\ &= (\delta - V)a_1^\dagger a_1 + (\delta + V)a_{-1}^\dagger a_{-1} \\ &\quad - V_{\text{ex},1}\hat{\sigma}_z a_1^\dagger a_1 + V_{\text{ex},-1}\hat{\sigma}_z a_{-1}^\dagger a_{-1} \\ &\quad + i\sqrt{\gamma_t}\frac{f_0}{\sqrt{2}}(a_1^\dagger - a_1) + i\sqrt{\gamma_t}\frac{f_0}{\sqrt{2}}(a_{-1}^\dagger - a_{-1}).\end{aligned}\quad (24)$$

Using the above Hamiltonian and following the procedure outlined in ref. 6 and we can derive the phase angles for a single-sided cavity as:

$$\begin{aligned}\tan(\theta_+) &= \frac{f_+ - f_+^*}{f_+ + f_+^*} = \frac{\gamma(\delta + V \pm V_{\text{ex},1})}{\frac{\gamma^2}{4} - (\delta + V \pm V_{\text{ex},1})^2}, \quad \text{and} \\ \tan(\theta_-) &= \frac{f_- - f_-^*}{f_- + f_-^*} = \frac{\gamma(\delta - V \mp V_{\text{ex},-1})}{\frac{\gamma^2}{4} - (\delta - V \mp V_{\text{ex},-1})^2}.\end{aligned}$$

Thus, we see that if  $U \ll \gamma$  the phase response will not be affected much. However, if  $U \gg \gamma$ , then the maximum of the signal is obtained when  $\delta = \pm V$  and the strength of the signal is reduced by half. This can be understood from a cartoon diagram in Fig. 2, which shows the  $J = 1$  and  $J = -1$  LP energy with respect to the probe detuning (horizontal axis). The solid lines represent the Lorentzian lineshape of the  $J = 1$  and  $J = -1$  LPs with width  $\gamma$  in the absence of QD electron. The dashed lines represent the shifted lineshapes when the QD spin state is  $\frac{1}{2}$ . If  $U \gg \gamma$  then at  $\delta = 0$ , the probe pulse is far detuned from either resonances. However, at  $\delta = V(-V)$ , it receives a maximum response from either of the  $J = 1$  or  $J = -1$  LPs. As a result the signal is reduced to half. For example at  $\delta = U$  and  $U \gg \gamma$ ,  $\theta_+ \sim 0$ ,  $\theta_- \sim \mp \frac{4V_{\text{ex},-1}}{\gamma}$ . Note that we must make a measurement at high  $\delta$  in order to reduce the crosstalk error due to polariton tunnel coupling with neighboring traps. For  $\delta \gg V$ , the signal will be independent of  $U$ . Hence for  $\delta = 0.3$  meV and  $U = 0.05$  meV, the shot-noise limited measurement time is  $\sim 660$  ps.

## VI. EFFECT OF POLARIZATION PINNING ( $V_s \neq 0$ ) ON TWO-QUBIT AND SINGLE-QUBIT GATE OPERATIONS

As described in the paper a  $\sigma_+(\sigma_-)$  polarized pump is required to excite  $J = 1$  ( $J = -1$ ) LPs for implementing a two-qubit (single-qubit) gate. However, because  $V_s \neq 0$ , the  $J = 1$  ( $J = -1$ ) LPs can be scattered into  $J = -1$  ( $J = 1$ ) LPs. As we know, the  $J = 1$  and  $J = -1$  experience opposite effects from their exchange interaction with the QD electron. Hence, a presence of both these polarization modes can be detrimental for the gate scheme. In this section we will derive the expressions in section V of the main paper and show that a non-zero  $V_s$  will have a negligible effect on the fidelity or gate time of the two- and single-qubit operations. Suppose a pump excites  $J = 1$  LPs in trap  $\ell$ , then in the absence of the QD electron, the Hamiltonian of the system is:

$$\begin{aligned}\hat{H} &= (\delta_\ell - V)a_{1,\ell}^\dagger a_{1,\ell} + (\delta_\ell + V)a_{-1,\ell}^\dagger a_{-1,\ell} \\ &\quad + V_s(a_{1,\ell}^\dagger a_{-1} + a_{-1}^\dagger a_{1,\ell}) - i\sqrt{\gamma_t}P(a_{1,\ell} - a_{-1,\ell})\end{aligned}\quad (25)$$

We will now drop the subscript  $\ell$  for clarity. Following the analysis in section V of the supplement we can derive the rate equations for the coherent state  $\alpha = \langle a_1 \rangle$  and  $\beta = \langle a_{-1} \rangle$ :

$$\begin{aligned}\frac{d\alpha}{dt} &= -i(\delta - V)\alpha - iV_s\beta - \frac{\gamma}{2}\alpha + \sqrt{\gamma_t}P \\ \frac{d\beta}{dt} &= -i(\delta + V)\beta - iV_s\alpha - \frac{\gamma}{2}\beta\end{aligned}\quad (26)$$

It will be instructive to solve the above equation at steady-state and assuming  $|\beta| \ll |\alpha|$ :

$$\begin{aligned}\Rightarrow |\alpha|^2 &\sim \frac{\gamma_t P^2}{(\delta - V)^2 + \frac{\gamma^2}{4}} = N \\ |\beta|^2 &\sim \frac{V_s^2}{(\delta + V)^2 + \frac{\gamma^2}{4}} |\alpha|^2\end{aligned}\quad (27)$$

Hence the fraction of  $J = -1$  LPs when the pump is  $\sigma_+$  polarized is  $\sim \frac{V_s^2}{(\delta + V)^2 + \frac{\gamma^2}{4}}$ . Similarly we can derive that the fraction of  $J = 1$  LPs when the pump is  $\sigma_-$  polarized is  $\sim \frac{V_s^2}{(\delta - V)^2 + \frac{\gamma^2}{4}}$ .

## REFERENCES

- 
- <sup>1</sup> D. Sarchi, I. Carusotto, M. Wouters, and V. Savona, *Phys. Rev. B* **77**, 125324 (2008)
  - <sup>2</sup> H. J. Carmichael, *Statistical Methods in Quantum Optics 1 Master Equations and Fokker-Planck Equations* Springer-Verlag Berlin Heidelberg (1999).
  - <sup>3</sup> V. Savona, L. C. Andreani, P. Schwendimann, and A. Quattropani, *Solid. State Commun.* **93**, 733 (1995)

<sup>4</sup> L. C. Andreani, G. Panzarini, and J. -M. Gérard, *Phys. Rev. B* **60**, 13276 (1999)

<sup>5</sup> D.F. Walls and G. J. Milburn, *Quantum Optics* (Springer-Verlag Berlin Heidelberg New York, 2000)

<sup>6</sup> S. Puri, P. L. McMahon, and Y. Yamamoto arXiv:1310.4873